ADVANCING EARTH AND SPACE SCIENCES

Tectonics

RESEARCH ARTICLE
10.1029/2025TC009333

Yiming Zhang and Eben Blake Hodgin these authors contributed equally to this work.

Key Points:

- High-grade Grenvillian metamorphism in the Adirondack Highlands persisted into the Rigolet phase, until at least 996 Ma
- Rutile and apatite U-Pb thermochronometry synthesized through probabilistic inversion reveal protracted post-Grenvillian cooling
- A younger magnetite remanence age shows Laurentia reached high southerly latitudes ca. 887 Ma, consistent with being equatorial ca. 990 Ma

Supporting Information:

Supporting Information may be found in the online version of this article.

Correspondence to:

Y. Zhang,
yiming-z@umn.edu

Citation:

Zhang, Y., Hodgin, E. B., Schmitz, M. D., Schwartz, D. M., Mohr, M. T., Crowley, J. L., & Swanson-Hysell, N. L. (2026). Protracted high-grade metamorphism and slow cooling in the Adirondacks recalibrate Neoproterozoic global paleogeography. *Tectonics*, *45*, e2025TC009333. https://doi.org/10.1029/2025TC009333

Received 12 DEC 2025
Accepted 25 MAY 2026

Author Contributions:

Conceptualization: Yiming Zhang, Eben Blake Hodgin, Nicholas L. Swanson-Hysell
Data curation: Yiming Zhang, Eben Blake Hodgin, Mark D. Schmitz, Darin M. Schwartz, Michael T. Mohr, James L. Crowley
Formal analysis: Yiming Zhang, Eben Blake Hodgin, Mark D. Schmitz, Darin

Protracted High-Grade Metamorphism and Slow Cooling in the Adirondacks Recalibrate Neoproterozoic Global Paleogeography

Yiming Zhang[1], Eben Blake Hodgin[2], Mark D. Schmitz[3], Darin M. Schwartz[3], Michael T. Mohr[3], James L. Crowley[3], and Nicholas L. Swanson-Hysell[1]

[1]Department of Earth & Environmental Sciences, Institute for Rock Magnetism, University of Minnesota Twin Cities, Minneapolis, MN, USA, [2]Department of Earth, Environmental & Planetary Sciences, Brown University, Providence, RI, USA, [3]Isotope Geology Lab, Department of Geosciences, Boise State University, Boise, ID, USA

Abstract The assembly and breakup of the supercontinent Rodinia set the stage for Earth system evolution through the Neoproterozoic Era. Laurentia, the central craton in Rodinia, lacks well-dated paleomagnetic poles between ca. 990 Ma and 780 Ma. In this study, we develop new U-Pb petrochronology and thermochronology data sets from zircon, garnet, titanite, rutile, and apatite from the Adirondack Highlands of the Grenville orogen. Data from zircon, garnet, and titanite show protracted high-grade metamorphism that lasted through ca. 996 Ma. Probabilistic thermal history modeling based on U-Pb cooling ages tightly constrains that the Adirondack Highlands slowly exhumed throughout the Neoproterozoic. The thermal history indicates that the paleomagnetic remanence records carried by titanomagnetite in Marcy massif anorthosite of the Adirondack Highlands were acquired ca. 887 ± 23 Ma—85 Myr later than previously estimated. In the context of existing late Mesoproterozoic and late Tonian apparent polar wander paths of Laurentia, our new data fill in a critical gap and imply that Rodinia was a slowly drifting supercontinent in the early to mid-Tonian.

Plain Language Summary The continental collision of the Grenvillian orogeny played a central role in assembling the supercontinent Rodinia a billion years ago. Magnetic records preserved in metamorphic rocks that cooled after mountain building are key to reconstructing Rodinia's position. Using multiple radiometric clocks, we show that metamorphism in the orogenic interior lasted longer and cooling was more protracted than previously recognized. Thermal history modeling reveals that the Marcy Massif in the Adirondack Highlands cooled slowly through mid-crustal temperatures around 880 million years ago, when magnetite-bearing rocks acquired magnetization. This revised timeline shifts a key paleomagnetic pole about 85 million years younger, resolving a major paleogeographic discrepancy concerning Rodinia's position.

1. Introduction

Reconstructing the position of ancient North America, Laurentia, is crucial to our understanding of global tectonics, geodynamics, and climate through the Neoproterozoic Era, particularly given its central location in the Rodinia supercontinent (e.g., Hoffman, 1991; Li et al., 2008). Currently, there exists a robust framework for Laurentia's paleogeography in the late Mesoproterozoic, but there remains paleogeographic uncertainty through much of the Neoproterozoic Era prior to the latest Tonian Period (ca. 780 to 719 Ma). Most late Mesoproterozoic constraints come from paleomagnetic data developed from magmatic rocks of the ca. 1.1 Ga North American Midcontinent Rift. The well-preserved thick successions of volcanic rocks have enabled high-resolution paleogeography reconstruction for Laurentia ca. 1109–1083 Ma through the Keweenawan Track sequence of paleomagnetic poles (e.g., Palmer & Davis, 1987; Swanson-Hysell et al., 2019). However, following the ca. 1083 Ma cessation of magmatism in the rift (Fairchild et al., 2017), there was a quiescence of intracratonic magmatic activity in Laurentia that lasted until the emplacement of the ca. 780 Ma Gunbarrel large igneous province (Harlan et al., 2003; Mackinder et al., 2019; Milton et al., 2017). In addition, there was limited basin development until the supercontinent began to break up, which also initiated ca. 780 Ma. As a result, there are few rock records in the interior of the supercontinent from which paleomagnetic records can be developed for the reconstruction of its early to mid-Tonian paleogeography (Li et al., 2008; Macdonald et al., 2023).

The need for quantitative paleogeographic constraints to reconstruct the position of Laurentia led researchers to exploit magnetizations acquired by metamorphic rocks during cooling within the Grenville orogen. Decades of

M. Schwartz, Michael T. Mohr, James L. Crowley, Nicholas L. Swanson-Hysell
Funding acquisition: Yiming Zhang, Eben Blake Hodgin, Mark D. Schmitz, Nicholas L. Swanson-Hysell
Investigation: Yiming Zhang, Eben Blake Hodgin, Mark D. Schmitz, Darin M. Schwartz, Michael T. Mohr, James L. Crowley, Nicholas L. Swanson-Hysell
Methodology: Yiming Zhang, Eben Blake Hodgin, Mark D. Schmitz, Nicholas L. Swanson-Hysell
Project administration: Mark D. Schmitz, Nicholas L. Swanson-Hysell
Resources: Yiming Zhang, Mark D. Schmitz, Nicholas L. Swanson-Hysell
Software: Yiming Zhang
Supervision: Mark D. Schmitz, Nicholas L. Swanson-Hysell
Validation: Yiming Zhang, Mark D. Schmitz
Visualization: Yiming Zhang, Eben Blake Hodgin
Writing – original draft: Yiming Zhang, Eben Blake Hodgin, Nicholas L. Swanson-Hysell
Writing – review & editing: Mark D. Schmitz, Darin M. Schwartz

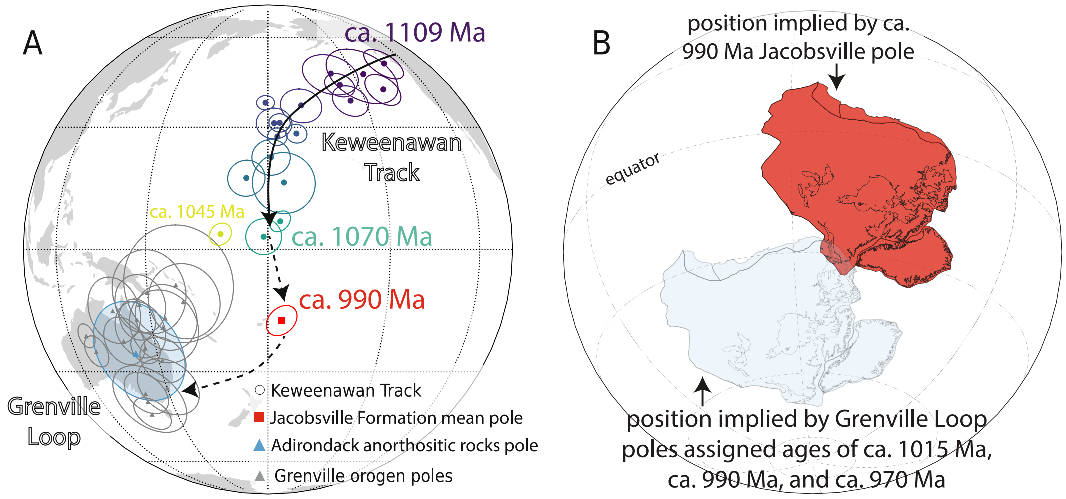

Figure 1. Late Mesoproterozoic to Neoproterozoic paleogeographic constraints for Laurentia. (a) Summary apparent polar wander path for Laurentia, including the ca. 1109–1083 Ma Keweenawan Track which loops down from northern high latitudes toward the equator (Swanson-Hysell et al., 2019). Recent sedimentary paleomagnetic data and associated chronostratigraphic constraints from Slotznick et al. (2023), Fuentes et al. (2025) extend the Keweenawan Track to ca. 1070–1045 Ma. The ca. 990 Ma Jacobsville Formation pole (Zhang, Hodgin, et al., 2024) and a compilation of paleomagnetic poles developed from metamorphic rocks of the Grenville Province (Halls, 2015) are shown. The pole position developed from anorthositic rocks from the Adirondack Highlands is shown in blue (L. Brown & McEnroe, 2012). (b) Apparently discrepant paleogeographic positions of Laurentia implied by the ca. 990 Ma Jacobsville pole (Zhang, Hodgin, et al., 2024) and Grenville poles with estimated ages of ca. 1015 Ma (Warnock et al., 2000), 990 Ma, and 970 Ma (L. Brown & McEnroe, 2012).

paleomagnetic research have shown that many granulite facies metamorphic rocks in the orogen carry stable magnetic remanence (e.g., Berger et al., 1979; L. Brown & McEnroe, 2012; Hargraves & Burt, 1967; McWilliams & Dunlop, 1975; Warnock et al., 2000). Geochronology data and paleomagnetic field tests have shown that the timing of magnetic remanence acquisition in those rocks postdates Grenvillian peak metamorphism (e.g., Berger et al., 1979; McWilliams & Dunlop, 1975; Warnock et al., 2000). Currently, there is a rich archive of paleomagnetic poles from Grenville rocks that cluster in a position significantly south of the end of the Keweenawan Track (Figure 1a). The observation that Laurentia's apparent polar wander path appears to loop south from the Keweenawan Track to the Grenville poles and then back up north again to late Tonian paleomagnetic poles (Figure 1a) has led to it being referred to as the "Grenville Loop" (Berger et al., 1979). In curated paleogeography databases (e.g., Evans et al., 2021; Li et al., 2008; Weil et al., 1998), reconstructions of Rodinia are heavily reliant on these Grenville Loop pole positions and their associated age estimates, both in terms of the supercontinent's absolute position and the relative configuration between Laurentia and its conjoined continents.

Constraining the ages and associated uncertainties of paleomagnetic records in high-grade metamorphic rocks is a challenging task. Given that the acquisition of remanent magnetization by magnetite in those rocks occurs during slow cooling through blocking temperatures (e.g., below Curie temperature of 580°C for magnetite), dating the timing of remanence acquisition in Grenville orogen metamorphic rocks requires reconstruction of the post-orogenic cooling history. Ideally, such a reconstruction should integrate a suite of petrochronometers and thermochronometers spanning a wide range of temperatures. This cooling history is also key for constraining rocks with hematite magnetizations where remanence was acquired during hematite–ilmenite exsolution at temperatures less than ∼520°C (L. Brown & McEnroe, 2012; Harrison, 2006; McEnroe et al., 2007). Warnock et al. (2000) developed paired paleomagnetic data and thermal history reconstructions from the Haliburton Highlands of the Central Metasedimentary Belt, Ontario, providing a pole position from magnetite-held magnetization with an estimated age of ca. 1015 Ma, which has been rated as a reliable constraint for Laurentia's paleogeography at the time (Figure 1a; Evans et al., 2021; Li et al., 2008). L. Brown and McEnroe (2012) correlated the exhumation history of magnetite-bearing anorthositic rocks of the Marcy Massif in the Adirondack Highlands with the thermal history paths for the region developed by Mezger et al. (1991), and estimated the age of the pole to be ca. 970 Ma. These paleomagnetic poles imply a high-latitude position for Laurentia in the southern hemisphere at the time that the magnetization was acquired (Figure 1).

Recently, a paleomagnetic pole combined with new chronostratigraphic data from the ca. 990 Ma sedimentary Jacobsville Formation in the interior of Laurentia offered new constraints on Rodinia's configuration in the early Tonian, revealing it to have been straddling the equator (Figure 1; Hodgin et al., 2022; Zhang, Hodgin, et al., 2024). This pole combined with constraints from the ca. 1075 to 1045 Ma Freda Formation (Fuentes et al., 2025) and the preceding Keweenawan Track reveals that Laurentia rapidly moved toward the equator ca. 1110 to 1080 Ma leading up to the Grenvillian orogeny, and significantly slowed down with the onset of collisional orogenesis (Figure 1).

It is a conundrum that the Grenville Loop poles imply high-latitude positions for Laurentia but were assigned ages that are both older and younger than the well-dated Jacobsville pole which implies a much lower latitudinal position (Figure 1b). Taking the previously assigned ages for the Grenville poles at face value, it has been interpreted that the Grenville orogen terranes were allochthonous to Laurentia at the onset of the orogeny, and experienced ∼4,000 km of transport relative to the continent associated with crustal shortening within the Grenville orogen (Halls, 2015). Others have posited that the Grenville Loop represents rapid true polar wander in the latest Mesoproterozoic (e.g., Evans, 2003). Zhang, Hodgin, et al. (2024) proposed another alternative explanation—the Grenville poles are much younger than previously estimated, and they record Laurentia's paleogeography well after ca. 990 Ma.

In this study, we test these hypotheses by quantitatively reconstructing the post-Grenville thermal history of the Marcy Massif anorthosite complex, New York (Figure 2). We developed zircon and titanite U-Pb data with paired trace element data, garnet U-Pb data, and rutile and apatite U-Pb thermochronology data. The zircon, garnet, and titanite data provide constraints on the timing and temperature of late-stage Grenvillian metamorphism. The high-precision rutile and apatite U-Pb data constrain the exhumation history of the anorthosite complex through mid-crustal levels. Using these data, we recalibrate the duration of high-grade metamorphism in the region and the timing when magnetite-bearing anorthositic rocks within the Marcy Massif acquired paleomagnetic remanence during exhumation.

2. Geological Background

The bedrock geology of the Adirondack region of New York state, USA can be generally divided into the Adirondack Highlands and the Adirondack Lowlands based on metamorphic grades (Figure 2; e.g., McLelland, Selleck, & Bickford, 2010). The highlands are dominated by ca. 1160 Ma anorthosite-mangerite-charnockite-granite (AMCG) intrusive suite rocks (McLelland et al., 2004). Geochronologic and geochemical data show that the AMCG units are associated with the ca. 1190–1160 Ma Shawinigan orogeny and experienced granulite facies metamorphism during the ca. 1090–980 Ma Grenvillian orogeny (e.g., Heumann et al., 2006; McLelland et al., 1988; Valley et al., 1994). Swanson-Hysell et al. (2023) compiled literature metamorphic zircon and monazite U-Pb dates across the Grenville orogen and analyzed their distributions. The data show a broad age range of Grenville metamorphism ca. 1090–980 Ma, with age populations clustering in two phases ca. 1090–1020 Ma and 1010–980 Ma, consistent with previously hypothesized Ottawan and Rigolet orogenic phases (Rivers, 2008). During the ca. 1090–1020 Ma Ottawan orogenic phase, it is estimated that peak metamorphism in the Adirondack highlands reached up to 950°C–1025°C (e.g., Metzger et al., 2021; Shinevar et al., 2021) and 1–1.2 GPa (e.g., Bohlen et al., 1985; Metzger et al., 2021; Spear & Markussen, 1997; Storm & Spear, 2005). It has been interpreted that such high-grade metamorphism resulted in extensional collapse of the overthickened and overheated crust during the late Ottawan phase, causing exhumation, deformation, and widespread metasomatism in the region (e.g., Regan et al., 2019; Rivers et al., 2012). It has also been interpreted that metamorphism associated with the ca. 1010–980 Ma Rigolet orogenic phase was significant in the western Grenville Province close to the Grenville Front (i.e., the Parautochthonous Belt; Figure 2), but had minimal impact in the hinterland of the orogen such as the Adirondack region (Rivers, 2008; Williams et al., 2019). The relatively sparse Rigolet-aged geochronology records in the Adirondack region have been interpreted to indicate minor crustal reheating and non-deformational metamorphism (e.g., Aleinikoff et al., 2021).

The Marcy Massif is the largest anorthositic body in the Adirondack Highlands with an exposed area of ∼3,000 km^2 (Figure 2). It is dominated by anorthosite to gabbroic anorthosite (McLelland et al., 2004). The

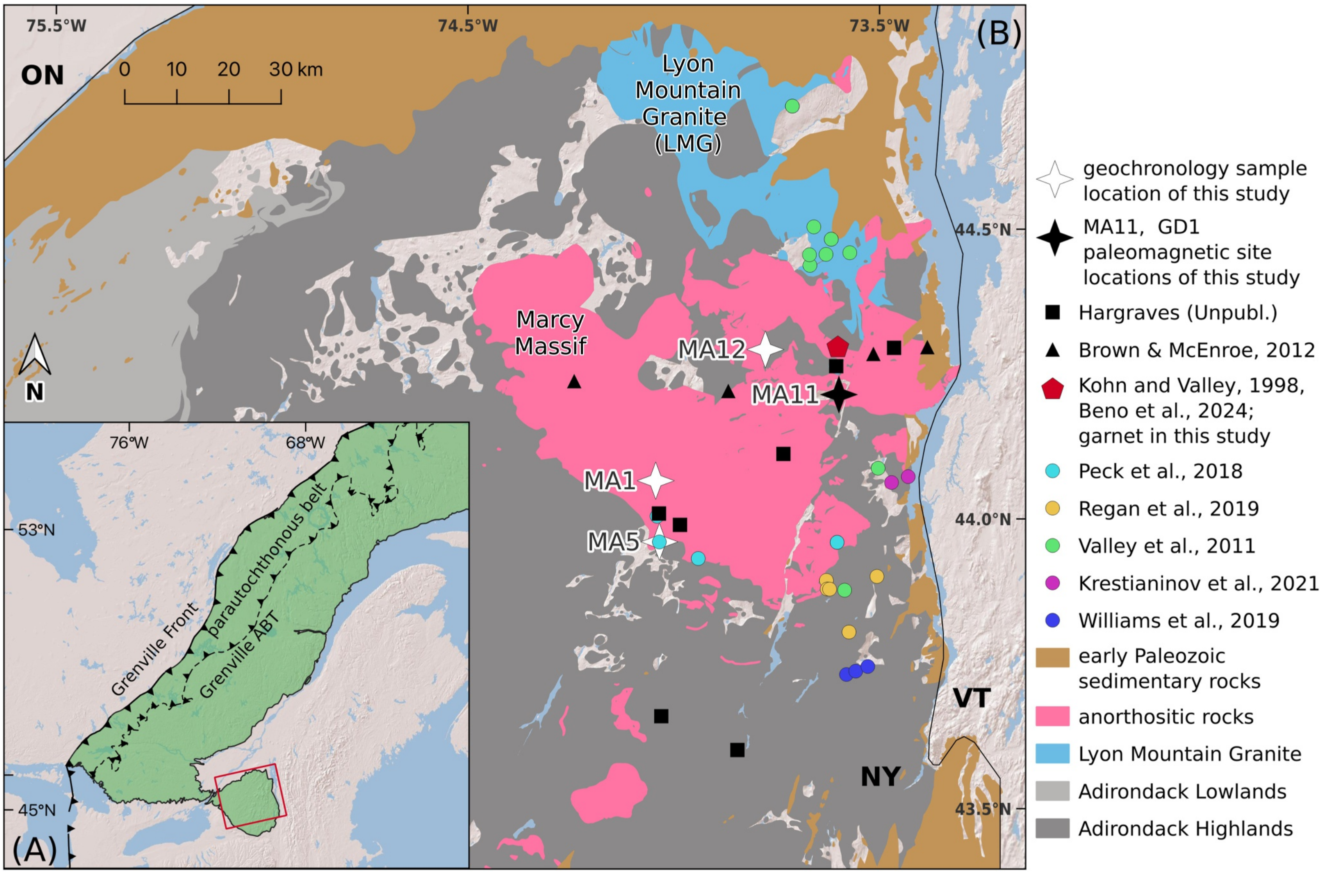

Figure 2. (a) Simplified map of the Grenville orogen in North America. The inferred extent of the Grenville Front (solid line) and the Grenville Allochthonous Boundary Thrust (ABT; dashed line) are shown with ticks on the hanging walls. They divide the Grenville Province into the Parautochthonous Belt and the Allochthonous Belt. The red box shows the extent of map (b). (b) Simplified bedrock geologic map of the Adirondack region, New York, USA (Dicken et al., 2005). Rocks of the Adirondack Highlands experienced up to granulite facies metamorphism, whereas those in the Lowlands typically experienced up to amphibolite facies metamorphism (Bohlen et al., 1985). The Marcy Massif anorthosite complex and the Lyon Mountain Granite (LMG) are highlighted. Marcy Massif geochronology sample locations MA1, MA5, and MA12 from this study are plotted. The paleomagnetic site MA11 is baked by a 9-cm-wide mafic dike GD1. Previous paleomagnetic sample localities of L. Brown and McEnroe (2012) are shown (estimated site locations of R.B. Hargraves were obtained by L. Brown and McEnroe (2012) via personal communication). Locations of notable geochronology samples from previous studies (Beno et al., 2024; Buchanan, 2015; Krestianinov et al., 2021; Peck et al., 2018; Regan et al., 2019) are shown. The exposed Cambrian-early Ordovician sedimentary rocks on the flank of the Adirondack Mountains are shown. ON—Ontario; NY—New York; VT—Vermont.

interior of the Marcy Massif mostly consists of these anorthositic lithologies where rocks typically exhibit igneous contact relationships, coarse textures, and preserve abundant plagioclase megacrysts ("Marcy facies"; Miller & Alling, 1918). Near the border of the massif, the lithologies can be more gabbroic with garnet-pyroxene reaction rims (coronas), and have more pronounced deformation fabrics and hydrothermal alteration ("Whiteface facies"; Kemp, 1898).

Numerous unmetamorphosed mafic dikes in the Adirondack region are known to postdate Grenvillian orogenesis. They crosscut the Marcy Massif but do not crosscut Paleozoic sedimentary rocks (Fisher, 1977). In southern Ontario and Québec, similarly E-W trending mafic dikes that crosscut Grenville rocks have been dated to be of Ediacaran age (Halls et al., 2015; Hyodo & Dunlop, 1993; Kamo et al., 1995).

3. Results and Interpretations

Geochronology sample MA1 is a Marcy facies sample collected in the interior of the Marcy Massif, ~10 km from the southern margin (44.07678°N, 74.05689°W; Figure 2). Petrographic data show that this sample has a granoblastic texture where plagioclase feldspar crystals are typically equigranular. Some plagioclase feldspar crystals exhibit deformation twinning (Figure S1 in Supporting Information S1). The sample contains pyroxene, quartz, rutile, magnetite, ilmenite, zircon, and apatite. Geochronology sample MA5 (43.97118°N, 74.04978°W) was collected from a Whiteface facies garnet-bearing leucogabbro near the southern border of the massif. Garnet crystals commonly contain abundant apatite inclusions (Figure S1 in Supporting Information S1). Sample MA12 was collected in the northern Marcy Massif (44.30080°N, 73.78959°W; Figure 2) from a gabbroic zone within a Marcy facies outcrop that contains blue-gray feldspar megacrysts. Zircon, apatite, and rutile grains were extracted from sample MA1; zircon and apatite grains were extracted from sample MA5; titanite grains were extracted from MA12. Standard mineral separation procedures were followed for all samples. Details of mineral separation and geochronology methods are presented in the Supporting Information. We also obtained garnet samples from the Willsboro-Lewis wollastonite deposit at the same location as reported in Beno et al. (2024) (Figure 2). The wollastonite deposit is in contact with the Marcy Massif and underwent granulite facies metamorphism during Grenvillian orogenesis (Clechenko & Valley, 2003; Valley et al., 1990).

We collected dike orientation data from two dikes that intrude the Marcy Massif. We collected oriented paleomagnetic samples from a 9-cm-thick dike (site GD1) and from the anorthosite host rock (site MA11; Figure 2) 1.5–24.0 cm away from the dike. These samples are used for a paleomagnetic baked contact test for relative dating of the timing of paleomagnetic remanence acquisition by the anorthosite host rock with respect to the emplacement of the dike. Detailed descriptions of sample preparation and paleomagnetic methods are presented in the Supporting Information.

3.1. Zircon U-Pb Geochronology and Geochemistry

A total of 15 zircon grains from sample MA1 and 42 zircon grains from MA5 were selected to be imaged with cathodoluminescence (CL) and dated with laser ablation-inductively coupled plasma-mass spectrometry (LA-ICP-MS; analytical details are in the Supporting Information S1) (Figures S2 and S3 in Supporting Information S1). Trace element concentrations were collected along with U and Pb isotope ratios during the analyses (Table S1 in Supporting Information S1). We calculated Ti-in-zircon thermometry values for each spot analysis (Figures S2 and S3 in Supporting Information S1; Ferry & Watson, 2007). The individual grain analyses show concordant or nearly concordant results with a spread of dates ca. 1200 to 1000 Ma (Figures S2 and S3 in Supporting Information S1). Subsequently, 10 grains from MA1 and 8 grains from MA5 were selected to be dated to higher precision through chemical abrasion-isotope dilution-thermal ionization mass spectrometry (CA-ID-TIMS). Results for individual grains are reported in Table S2 of Supporting Information S1. The CA-ID-TIMS analyses also show a spread of apparent $^{206}Pb/^{238}U$ dates that range from 1159.73 ± 0.92 Ma to 995.81 ± 0.74 Ma (all ID-TIMS date uncertainties presented in this study are 2σ analytical uncertainties). The data reveal that many grains have discordant dates despite having undergone chemical abrasion before ID-TIMS analysis (Figures 3a and 3b). Our interpretation of the crystallization age of the Marcy anorthosite and the protracted high-grade metamorphism history recorded by these zircon dates is summarized in Figure 3c.

Zircon grains MA1-z6 and two fragments of grain MA1-z10 yielded concordant CA-ID-TIMS analyses with $^{206}Pb/^{238}U$ dates of 1158.90 ± 0.57 Ma, 1158.70 ± 0.92 Ma, and 1159.73 ± 0.92 Ma (Figure 3a). These dates overlap, and they all overlap with the previous weighted mean age of 1155 ± 5 Ma from in situ zircon U-Pb analyses developed by McLelland et al. (2004) from the Marcy Massif within uncertainty. In sample MA5, the oldest zircon CA-ID-TIMS $^{206}Pb/^{238}U$ date is 1150.87 ± 0.90 Ma and the youngest date is 995.81 ± 0.74 Ma (Figure 3b and Table S2 in Supporting Information S1). Overall, our data support a petrogenetic model in which Marcy Massif plutonism occurred ca. 1160 Ma, during the latest stage of the ca. 1190–1160 Ma accretionary Shawinigan orogeny (e.g., Chiarenzelli et al., 2010; McLelland, 2016; McLelland, Selleck, Hamilton, & Bickford, 2010; Peck et al., 2013; Swanson-Hysell et al., 2023; Valentino et al., 2019).

The CA-ID-TIMS dates from other dated zircons in both MA1 and MA5 indicate protracted high-grade metamorphism during the Grenvillian orogeny. These include dates from grains MA1-z7, MA5-z5 and MA5-z6, whose anhedral shapes and lack of apparent zoning in CL imagery are consistent with them having crystallized during metamorphism (Figure S2 in Supporting Information S1). These zircon grains have $^{206}Pb/^{238}U$ dates of 1013.17 ± 0.65 Ma, 995.81 ± 0.74 Ma, and 1016.75 ± 0.68 Ma, respectively; and Ti-in-zircon temperature estimates of ∼690°C, ∼628°C, and ∼640°C, respectively (Figures S2 and S3 in Supporting Information S1). These temperatures are low compared to the igneous zircons which record temperatures up to ∼860°C (e.g., grain MA1-z6; Figure S2 and Table S1 in Supporting Information S1). Together, grains MA1-z7, MA5-z5, and MA5-z6 are consistent with having grown during metamorphism and indicate that there was protracted metamorphism in the Marcy

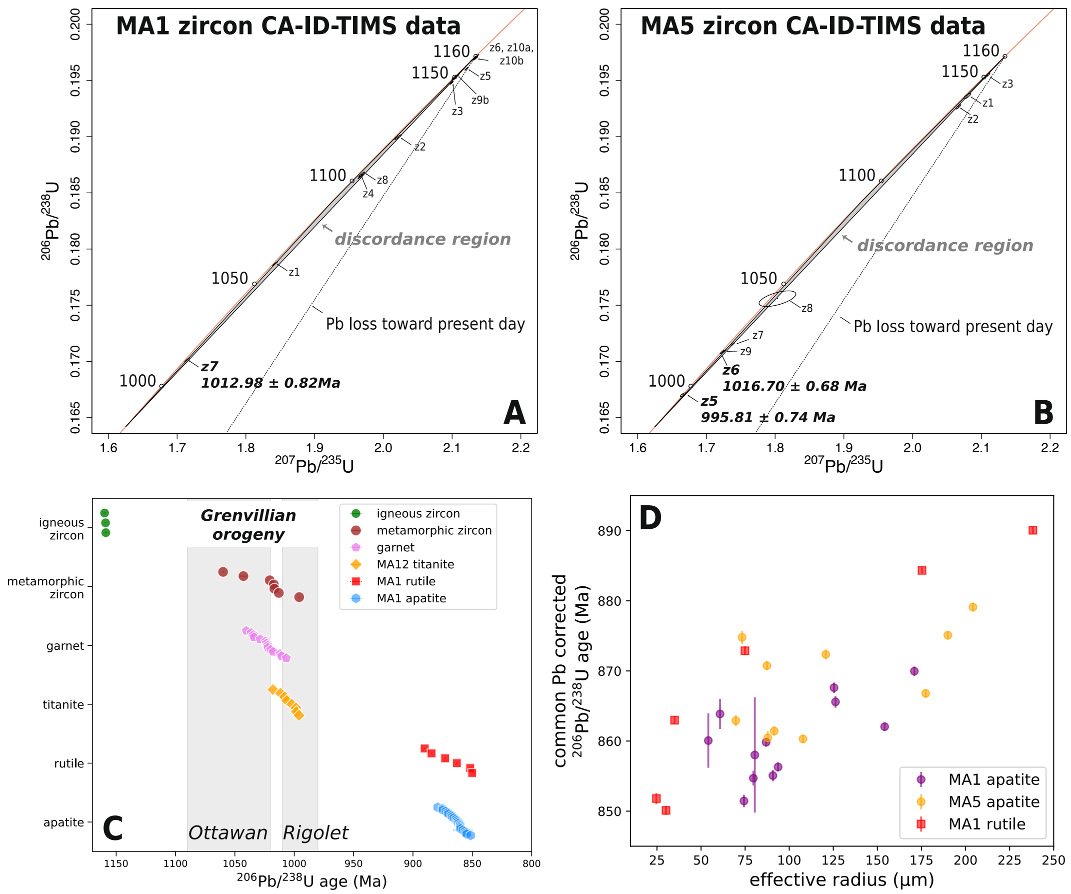

Figure 3. (a) Wetherill concordia diagram for the CA-ID-TIMS U-Pb zircon geochronology results for sample MA1. Grains z6 and two fragments of grain MA1-z10 underwent chemical abrasion at 220°C for 12 hr and yielded concordant analyses with $^{206}Pb/^{238}U$ dates of 1158.90 ± 0.57 Ma, 1158.70 ± 0.92 Ma, and 1159.73 ± 0.92 Ma. Grain z7 yielded the youngest $^{206}Pb/^{238}U$ date of 1012.98 ± 0.82 Ma (2σ). (b) Wetherill concordia diagram for the CA-ID-TIMS U-Pb zircon geochronology results for sample MA5. Grain z5 is concordant and yielded the youngest $^{206}Pb/^{238}U$ date of 995.81 ± 0.74 Ma (2σ) within the sample. The filled gray areas in both (a, b) illustrate plausible zircon U-Pb discordance in a scenario where they formed ca. 1160 Ma and underwent metamorphism during ca. 1090–980 Ma Grenvillian orogenesis. The dashed lines in both plots show the expected discordance trajectory caused by Pb loss at present day. (c) Summary plot of all U-Pb ID-TIMS geochronology data developed in this study. Initial emplacement of the Marcy Massif ca. 1159 Ma is constrained by overlapping concordant $^{206}Pb/^{238}U$ dates of 1158.90 ± 0.57 Ma, 1158.70 ± 0.92 Ma, and 1159.73 ± 0.92 Ma interpreted as igneous zircon crystallization. Grenvillian metamorphism timing is constrained by metamorphic zircon, garnet, and titanite dates. Abundant concordant and minimally discordant zircon dates from both MA1 and MA5 range from ca. 1050 to 996 Ma associated with Pb loss that was annealed and/or metamorphic crystallization–recording high-grade metamorphism conditions during the Grenvillian orogeny. A few discordant zircon analyses that have apparent $^{206}Pb/^{238}U$ dates younger than 1159 Ma, but older than 1100 Ma, are omitted (a). Rutile and apatite dates reveal slow cooling of the Marcy Massif through the mid-crustal levels. (d) Common Pb corrected $^{206}Pb/^{238}U$ dates of all rutile and apatite grains dated with ID-TIMS are plotted against their effective grain sizes. There is a grain size-age correlation where larger grains record older ages than smaller ones. This is consistent with the grains recording cooling ages. All age uncertainties are 2σ analytical uncertainties. Additional reference material ID-TIMS measurements are presented in Table S11 of Supporting Information S1.

Massif during the Rigolet phase of the Grenvillian orogeny. We interpret metamorphic zircon MA5-z5 to constrain that the Marcy Massif was at a temperature of 628 ± 30°C at 995.81 ± 0.74 Ma.

3.2. Garnet U-Pb Geochronology

U-Pb isotope ratios were measured via ID-TIMS for a total of 9 andradite garnet crystals from the Willsboro-Lewis skarn deposit in contact with the Marcy Massif (same sample as that of Kohn & Valley, 1998; Figure 2b). Garnet U-Pb isotope ratios were corrected using common Pb isotope measurements from cogenetic diopside in the skarn deposit (Beno et al., 2024), which yielded concordant and minimally discordant results with a range of $^{206}Pb/^{238}U$ dates ca. 1040 to 1007 Ma (Figure 3c and Figure S4, Table S3 in Supporting Information S1). This age range is similar to, but more protracted than, that obtained by Beno et al. (2024) from the same deposit. Given the lack of experimental constraints on Pb diffusivity in garnet, it is difficult to distinguish whether such young ages are due to recrystallization or diffusive Pb loss in the garnet. Regardless, the distribution of garnet U-Pb ages through ca. 1040 to 1007 Ma indicates that protracted, poly-phased, high-grade metamorphism in the Adirondack Highlands lasted for tens of millions of years through the late-Ottawan to Rigolet phase of the Grenvillian orogeny.

3.3. Titanite U-Pb Geochronology and Geochemistry

U-Pb isotope ratios and trace element concentrations of 35 titanite grains from sample MA12 in northern Marcy Massif (Figure 2) were measured with LA-ICP-MS (Figure S5 and Table S4 in Supporting Information S1). The grains have sufficient variation in the U-Pb ratios such that an isochron line fit could be made with the data on a Tera-Wasserburg diagram to determine a lower intercept age of 1000 ± 21 Ma (2σ analytical uncertainty; MSWD = 2.4; Figure S5 in Supporting Information S1). Subsequently, 8 of the same grains were dated in tandem by ID-TIMS (Figure 3c and Table S5 in Supporting Information S1). We also measured common Pb isotopic ratios from feldspar separates from the same sample in order to more accurately correct for common Pb in the titanite (Tables S5 and S10 in Supporting Information S1). The common Pb-corrected $^{206}Pb/^{238}U$ dates resolve distinct individual dates that range between 1017.91 ± 0.55 Ma and 995.95 ± 0.73 Ma (Figure 3c and Figure S4 in Supporting Information S1).

The high-precision ID-TIMS dates are within uncertainty of the Tera-Wasserburg diagram lower intercept age of 1000 ± 21 Ma from the LA-ICP-MS in situ data. These dates are younger than the ca. 1159 Ma crystallization age of the Marcy anorthosite, and are similar to the zircon and garnet U-Pb dates that record metamorphism through the late Ottawan to Rigolet orogenic phases (Figure 3c). However, the titanite grains record consistent REE patterns with minimal Eu depletion (Figure S5 in Supporting Information S1), and have higher Zr-in-titanite temperatures (95% confidence interval between 782°C and 860°C; Figure S5 and Table S4 in Supporting Information S1; Hayden et al. (2007)) than the Ti-in-zircon thermometry values recorded by zircons that have similar ages (Figures S2, S3 and Table S1 in Supporting Information S1). This result could indicate the passage of earlier high-temperatures of the titanite crystals through the partial retention zones of Zr and Pb diffusion (Cherniak, 1993, 2006). The titanite results support that there was high-temperature metamorphism in the northern part of the Marcy Massif (Figure 2) during the Rigolet phase of the Grenvillian orogeny.

3.4. Rutile U-Pb Geochronology and Geochemistry

Rutile grains were separated from sample MA1 (Figure 2). The larger grains are typically subhedral and opaque with metallic luster, while the smaller grains are typically euhedral, partially translucent, and red when observed under a binocular microscope. The grains were mounted on double-sided Kapton tape before imaging by backscattered electron microscopy (BSE) for grain size determination (Figure S6 in Supporting Information S1). The grains were not cast in epoxy and polished in order to preserve their original geometry and volume. U-Pb isotope ratios and trace element concentrations of 27 rutile grains were measured with LA-ICP-MS (Figure S6 and Table S6 in Supporting Information S1). Many grains have sufficient U and minimal common Pb such that the data are concordant or minimally discordant, with the concordant analyses showing a range of dates (Figure S6 in Supporting Information S1). We calculated the Zr-in-rutile thermometry values and associated uncertainties for the individual rutile grains (Kohn, 2020). In contrast to the tight distribution of Zr-in-titanite temperatures (Figure S6 in Supporting Information S1), the Zr-in-rutile temperature values show a broad distribution with distinct clusters of temperatures around 750°C and 950°C (Figure S6 in Supporting Information S1).

Subsequently, we selected six crystals with relatively high U concentration that have a grain size range of ~25–238 μm (effective grain radius calculated following R. W. Brown et al. (2013), Beucher et al. (2013)), and dated with ID-TIMS, including an initial common Pb isotope correction using feldspar from sample MA1 (Tables S7 and S10 in Supporting Information S1). These relatively radiogenic rutile grains produced $^{206}Pb/^{238}U$ dates insensitive to the common Pb correction, ranging between 890.08 ± 0.50 Ma and 850.11 ± 0.64 Ma (Figures 3c and 3d). These high-precision rutile ID-TIMS dates are significantly younger than the timing of Ottawan to Rigolet phase high-grade metamorphism recorded by zircon, garnet, and titanite (Figure 3c). When plotting the dates against grain sizes (Figure 3d), a correlation emerges—older dates are associated with larger grain sizes.

The pattern of younger dates in smaller grains indicates that Pb was lost by volume diffusion and that the rutile grains are recording cooling ages.

3.5. Apatite U-Pb Geochronology and Geochemistry

U-Pb isotope ratios along with trace element concentrations for apatite grains from MA1 and MA5 were mounted and measured with LA-ICP-MS (Figures S7, S8 and Table S8 in Supporting Information S1). Like rutile, apatite grains from samples MA1 and MA5 were mounted without casting and polishing to preserve their original geometry and volume. Based on the in situ measurement results, we found that the apatite grains in these samples are U-rich. Subsequently, apatite with various grain sizes were selected for ID-TIMS analyses (Table S9 in Supporting Information S1). As a result, a total of 33 grains from MA1 and 28 grains from MA5 were measured by LA-ICP-MS, and a total of 12 grains from MA1 and 10 grains from MA5 with a grain size range of ∼54–204 μm were dated by ID-TIMS (Figures 3c and 3d) with the results corrected for common Pb using coexisting feldspar common Pb isotopic ratios (Tables S9 and S10 in Supporting Information S1). There are five grains from MA1 and three grains from MA5 that were dated by ID-TIMS without being analyzed by LA-ICP-MS to preserve their original volumes.

Overall, the MA1 and MA5 apatite grains measured with ID-TIMS have sufficient radiogenic Pb such that their final U-Pb ratios are not very sensitive to common Pb correction (Figures S4, S7, S8 and Tables S9, S10 in Supporting Information S1). The apatite common Pb corrected $^{206}Pb/^{238}U$ dates range from 881.78 ± 1.47 Ma to 851.45 ± 0.90 Ma, which is similar to the range of the rutile ID-TIMS dates (Figure 3c). When plotting the dates against grain sizes (Figure 3d), the apatite data also show a grain size-age correlation, consistent with them having experienced volume diffusion and recording cooling ages. Additionally, apatite consistently record younger ages than the rutile grains of similar sizes (Figure 3d), consistent with experimental Pb diffusivities in apatite being faster than in rutile (Cherniak, 2000; Cherniak et al., 1991).

3.6. Paleomagnetic Baked Contact Test

L. Brown and McEnroe (2012) developed a paleomagnetic pole from the Marcy Massif anorthositic rocks and assigned an age of ca. 970 Ma based on associating the magnetic remanence unblocking temperature range with the thermal history developed by Mezger et al. (1991). Confidence in the pole position can be gained by its similar position to paleomagnetic poles developed from Grenville rocks in other parts of the orogen (Figure 1a). However, there is no existing direct paleomagnetic field test in these rocks that can constrain the age of the remanence as well as a lack of documentation of whether a post-Grenvillian structural correction is required in the region. We collected standard paleomagnetic core samples from a 9-cm-thick mafic dike (site GD1) that intrudes the host anorthosite (site MA11) for a baked contact test (Figure 2b and Figure S9 in Supporting Information S1). The paleomagnetic specimens were thermally demagnetized (Figure S9 in Supporting Information S1; experimental details are in the Supporting Information S1; http://doi.org/10.7288/V4/MAGIC/20549). Specimens from the mafic dike show a well-grouped component that sharply unblocks between ∼540°C and 560°C, after the removal of a low-temperature component that overlaps with the present-day dipole field direction in the region (Figure S9 in Supporting Information S1). The anorthosite samples MA11–1 and MA11-2 which are 1.5 and 4 cm away from the dike also record a SW and downward directional component that unblocks between ∼500–585°C. In sample MA11-3 which is 6 cm away from the dike, there is not only a SW and down component that unblocks between 569°C and 576°C, but also another component that unblocks ∼576°C–589°C with a distinct direction. The other 6 samples of MA11 are all more than 6 cm away from the dike, and their origin-trending component that typically unblocks between 570°C and 590°C is similar to the highest-temperature component of MA11-3. This unblocking temperature range is consistent with the magnetic remanence being held by low-Ti titanomagnetite (Dunlop & Özdemir, 2015). That MA11-1 and MA11-2 are completely baked by the dike, MA11-3 is partially baked, and the rest of the samples that are minimally baked by the dike but record a coherent directional group is a positive result for the paleomagnetic baked contact test. Given that the mafic dikes in the Adirondack area intrude Proterozoic rocks but not Paleozoic rocks (Fisher, 1977), this positive baked contact test result supports that the magnetic remanence held by titanomagnetite at site MA11 is Proterozoic in age. The origin-trending direction from the unbaked MA11 samples overlaps with the magnetite-carrying characteristic component direction developed from other sites of Marcy anorthosite rocks by L. Brown and McEnroe (2012) (Figure S9 in Supporting Information S1). Therefore, our positive baked contact test results support that the Marcy anorthosite paleomagnetic pole developed by L. Brown and McEnroe (2012) is an ancient pole acquired during post-orogenic cooling of the massif. Lastly, our dike plane orientation data collected from two mafic dikes that intrude the Marcy Massif are indistinguishable from vertical (Figure S9 in Supporting Information S1). These data are consistent with the Marcy Massif having experienced minimal tilting in the Phanerozoic Eon.

4. Discussion

4.1. Marcy Massif Petrochronology and Thermochronology

Zircon, garnet, titanite, rutile, and apatite are excellent mineral chronometers given that they incorporate uranium during crystallization. However, due to their different Pb retention capabilities, these minerals' U-Pb isotopic systems can serve as petrochronometers (i.e., record timing of crystal growth) and/or thermochronometers (i.e., constrain cooling history that postdates crystallization). It is well understood that crystalline zircon is highly retentive for both U and Pb (Cherniak et al., 1997; Cherniak & Watson, 2001) and is thus a faithful petrochronometer that records timing of zircon crystallization. However, metamictization caused by alpha decay, alpha recoil, and spontaneous fission processes can result in Pb-loss associated discordance in igneous zircons (e.g., Mattinson, 2005; Mezger & Krogstad, 1997). Fluid associated with metamorphism can lead to zircon re- and neo-crystallization such that single zircon crystals can have older cores recording igneous crystallization ages and younger metamorphic rims recording metamorphic ages. In this study, a zircon grain MA1-z6 was chemically abraded at 190°C for 12 hr, and yielded a $^{206}Pb/^{238}U$ date of 1158.9 ± 0.571 Ma. Two fragments of grain MA1-z10 were more intensely chemically abraded at 220°C for 12 hr. MA1-z10a yielded an age of 1158.7 ± 0.922 Ma and MA1-z10b yielded the oldest and concordant analysis of 1159.73 ± 0.92 Ma (Figure 3a and Table S2 in Supporting Information S1). A weighted mean age calculated with these three analyses is 1159.04 ± 0.42 Ma (MSWD = 1.5). The remaining zircons from sample MA1 were chemically abraded at 190°C. Although this approach often fully eliminates discordance associated Pb loss in igneous zircons (e.g., Mattinson, 2005), it did not fully mitigate discordance in those grains. All grains from sample MA5 were chemically abraded at 200°C. The results yielded apparent $^{206}Pb/^{238}U$ dates that span 1150.87 ± 0.90 Ma to 995.81 ± 0.74 Ma with variable discordance (Figure 3). The fact that intense chemical abrasion did not fully eliminate discordance in many zircon grains in both MA1 and MA5 indicates that Grenvillian metamorphism likely led to Pb loss in igneous zircons and thermally annealed the metamictized regions. It is also possible that the metamorphism led to volumetrically significant metamorphic zircon growth, even though our CL imaging shows that secondary rims are generally absent or very thin in some cases (Figures S2 and S3 in Supporting Information S1). Regardless of the origin of zircon discordance, all zircon analyses fall in a region defined by the ca. 1159 Ma Marcy crystallization age and ca. 1090–980 Ma Grenvillian orogenesis (Figures 3a and 3b). The U-Pb metamorphic zircon dates constrain that high-temperature conditions continued to at least 995.81 ± 0.74 Ma (Figure 3).

Grossular-andradite garnet and titanite have been demonstrated to be capable of incorporating trace amounts of U during formation (Dewolf et al., 1996) and be suitable for U-Pb geochronology studies (Beno et al., 2024; Seman et al., 2017). However, there are poor constraints on the diffusivities of U and Pb in garnet due to a lack of experimental measurements and field tests. Absolute titanite Pb closure temperatures are also somewhat uncertain due to inconsistencies among estimates based on various natural settings (generally higher temperatures, e.g., Gao et al., 2012; Kohn & Corrie, 2011; Mattinson, 1978) and experimental measurements (lower temperatures, Beyer et al., 2019; Cherniak, 1993), although the relative diffusivities of REE, Zr, and Pb are more confidently established (Cherniak, 2006). While these uncertainties make it challenging to confidently interpret the origin of the specific ages, our multichronometric analyses provide additional useful context. Tandem CA-ID-TIMS and LA-ICP-MS measurements on MA1 and MA5 zircon grains show that high-temperature metamorphism (>650°C) persisted from ca. 1050 Ma through to 996 Ma (Figure 3 and Figures S2, S3 in Supporting Information S1). Given that the garnet and titanite grains yielded dates that span a similar age range (Figure 3c), one interpretation would be that they are petrochronometers that record metamorphic crystallization during late-Ottawan to Rigolet phase metamorphism. However, this model cannot reconcile ~800°C Zr-in-titanite temperatures and ~650°C Ti-in-zircon values recorded by crystals of similar U-Pb ages (Figures S2, S3, S5 and Tables S1, S4 in Supporting Information S1). An alternative interpretation is thermochronological, whereby the titanite formed earlier and subsequently cooled through one or both of the Zr and Pb diffusion partial retention zones during late-stage Grenvillian metamorphism. Regardless, the array of precise ID-TIMS dates from Rigolet-aged garnet and titanite crystals adds to the evidence that protracted high-grade metamorphism continued to ca. 996 Ma in the Adirondack Highlands.

Rutile and apatite U-Pb systems are relatively well-characterized thermochronometers with moderate Pb retentivity. Experimental Pb diffusivities suggest that rutile has a nominal closure interval of ∼500°C–750°C and apatite ∼370°C–570°C, with the important context that these values are dependent on grain size and cooling rate (Cherniak, 2000; Cherniak et al., 1991). Our ID-TIMS data show that the Marcy rutile and apatite passed through their partial Pb retention zones ca. 890–850 Ma (Figures 3c and 3d). Those dates are ∼100–140 Myr younger than Grenvillian high-grade metamorphism recorded by zircon, garnet, and titanite (Figure 3c). Therefore, rutile and apatite cooling ages are parsimoniously interpreted as a consequence of thermal relaxation and exhumation in the Adirondack Highland region following peak Grenvillian metamorphism.

It is known that apatite can be prone to fluid-mediated reprecipitation and alteration associated with processes including retrograde metamorphism at temperatures lower than its nominal Pb closure temperatures (e.g., Corfu & Stone, 1998; Odlum et al., 2022; Schoene & Bowring, 2007). In those cases, the apatite U-Pb system should be treated as a petrochronometer instead of being used as a thermochronometer for constraining cooling histories. BSE images of our dated apatite grains show euhedral crystal shapes (Figures S7 and S8 in Supporting Information S1). In petrographic images, sample MA1 is dominated by large, granoblastic feldspar crystals with interstitial ameboid-shaped Fe-oxides (Figure S1 in Supporting Information S1). These data corroborate with observations made by McLelland et al. (1994), who presented geochemical data from Marcy anorthosite that support a petrogenetic model where the ameboid-shaped, intergranular oxides which enclose or occur adjacent to apatite grains were late-crystallizing mineral phases during fractional crystallization of a magma from which feldspar first crystallized. The consistent negative Eu anomaly in all MA1 apatite grains (Figure S7 in Supporting Information S1) also support that they crystallized as primary igneous minerals after feldspar crystallization which depleted Eu from the magma. In MA5, apatite are often enshrouded within larger garnet crystals which also have plagioclase inclusions (Figure S1 in Supporting Information S1). The occurrence of garnet in rocks near the margin of Marcy Massif is consistent with the petrologic model of McLelland and Whitney (1977), where garnet is a product of subsolidus reaction between anorthosite, Fe-oxides, olivine, and pyroxene. It is likely that the euhedral apatite in MA5 ended up being enclosed within garnet as metamorphism consumed primary minerals such as feldspar and oxides. Some apatite in MA5 are depleted in heavy REE when compared with those in MA1 (Figures S7 and S8 in Supporting Information S1). Such a pattern is likely associated with apatite re- or neo-crystallization during garnet formation (Thieblot et al., 1999). However, the garnet formation reactions had to happen at subsolidus conditions during Grenville peak metamorphism, where the apatite U-Pb system would have stayed open and subsequently cooled through closure temperatures during post-Grenville exhumation. In addition, there is no known evidence for Tonian large-scale tectonic or magmatic activity in the Adirondack Highlands that postdate the Grenvillian orogenesis (Selleck, 1980). Together with the grain size-age correlations, the ca. 880–860 Ma dates from the apatite crystals in this study are the most consistent with recording middle Tonian cooling ages.

Additionally, our multi-mineral U-Pb geochronology data set provides new insights on the mobility of Pb in the studied mineral chronometers. Previously, results of laboratory diffusion experiments suggest that Pb closure temperatures (Tc) are: $Tc_{rutile} > Tc_{titanite} > Tc_{apatite}$ (Cherniak, 1993, 2000; Cherniak et al., 1991). However, our data show that the rutile crystals have much younger dates than titanite (Figure 3c). These data indicate that Pb diffusivity in titanite is slower than that in rutile, or that diffusion is not the only process that can control Pb mobility in titanite (e.g., Garber et al., 2017). Large age discrepancies also exist between garnet and rutile dates (Figure 3c), indicating grossular-andradite garnet should have high Pb retention potential at high temperatures.

4.2. Grenvillian Metamorphism in the Adirondack Highlands and Its Impact in Interior Laurentia

Based on petrological, structural, and geochronological data, the ca. 1090–1020 Ma Ottawan phase of the Grenvillian orogeny is interpreted to have featured high-pressure (up to ∼1.2–1.7 GPa; e.g., Indares, 1993, 1995; Indares & Dunning, 1997; Rivers, 2008), high-temperature (exceeding 950°C; e.g., Metzger et al., 2021; Shinevar et al., 2021) metamorphism in the orogenic hinterland, resulting in crustal over-thickening and subsequent orogenic collapse (Indares, 2024; Rivers et al., 2012). Subsequently, during the Rigolet phase of the orogeny, contractional deformation is known to have been concentrated along the Grenville Front within the Grenvillian foreland (Figure 2), and to have propagated even further into the interior of Laurentia (e.g., Hodgin et al., 2022; Hynes & Rivers, 2010; Indares, 2024). However, metamorphism associated with the ca. 1010–980 Ma Rigolet phase of the orogeny has been interpreted to have involved only minor crustal reheating and non-deformational metamorphism in the Adirondack Highlands (e.g., Rivers, 2008; Williams et al., 2019). As a result, previous post-orogenic cooling estimates in the Adirondack Highlands typically considered the region to have monotonically cooled after Ottawan peak metamorphism ca. 1050 Ma (e.g., Mezger et al., 1991; Rivers, 2008).

Our new data indicate that high-grade metamorphism in the Adirondack region continued through the Rigolet phase of the Grenvillian orogeny. That older apparent Shawinigan and Ottawan-aged zircon do not define a single discordance trajectory suggests multiple and protracted episode(s) of Grenvillian metamorphism in the Adirondack Highlands (Figure 3). Zircon ages as young as 1017 to 996 Ma demand a complex metamorphism history in the Marcy Massif extending into the Rigolet phase of Grenvillian orogenesis. The interpretation that high-grade metamorphism continued during the Rigolet orogenic phase is further supported by our ca. 1040–1007 Ma U-Pb Willsboro-Lewis garnet dates and the ca. 1019–997 Ma MA12 U-Pb titanite dates (Figure 3c). This interpretation of protracted metamorphism in the Marcy Massif is further supported by additional in situ geochronology data from other units in the region. U-Pb zircon and monazite data developed by Regan et al. (2019) and Williams et al. (2019) show ca. 1010 to 980 Ma monazite rim dates from granite and gneiss lithologies southeast of the Marcy Massif (Figure 2). In the Lyon Mountain Granite northeast of Marcy (Figure 2), Buchanan (2015) and Aleinikoff et al. (2021) obtained in situ U-Pb zircon rim dates that range from 1060 to 1000 Ma and Buchanan (2015) obtained titanite U-Pb ID-TIMS dates of ca. 1000 Ma. These data corroborate previous interpretations of regional, high-grade, polycyclic metamorphism in the Adirondack region based on mineralogical and textural evidence (e.g., Bohlen et al., 1985).

Field and geochronology evidence constrain the Rigolet orogenic phase to have caused deformation in the western part of the Grenville orogen and further into Laurentia's interior. Syn-to late-deformational felsic leucosomes within the Grenville Parautochthonous Belt (Figure 2) have been dated to be ca. 1020–970 Ma (Jannin et al., 2018; Lambert et al., 2023; Pfister et al., 2023). The data indicate there was protracted suprasolidus deformation. Contractional deformation >500 km to the west of the Grenville Front within the orogenic foreland resulted in a final ca. 985 Ma episode of inversion of the Midcontinent Rift associated with the Rigolet phase (Hodgin et al., 2022, 2024). Syn-tectonic sedimentation of the ca. 995 Ma Jacobsville Formation and the Bayfield Group (Hodgin et al., 2022, 2024) post-dated an earlier episode of ca. 1040 Ma contractional deformation during the Ottawan orogenic phase in the continental interior that exhumed a thick panel of Archean basement to Midcontinent Rift volcanic rocks along thrust faults in the southern Lake Superior area (Cannon et al., 1993; Fuentes et al., 2025). Taken together, these data indicate that Rigolet phase orogenesis led to continued crustal thickening and metamorphism within the interior of the orogen, with associated lithospheric deformation propagating far into the midcontinent of Laurentia. The new data from the Adirondacks reveal that this stage of the orogeny also resulted in metamorphism in the interior of the orogen east of the Grenville Front.

4.3. Post-Grenville Thermal History of the Adirondack Highlands

There is an opportunity to develop a new quantitative, continuous post-Grenvillian thermal history for the Adirondack Highlands that integrates our new petrochronologic and thermochronologic constraints, including grain-size–age relationships. Existing treatments have largely relied on semi-quantitative estimates of average Tonian cooling rates from U–Pb and Ar data (e.g., Cosca et al., 1991; Dahl et al., 2004; Martignole & Reynolds, 1997; Mezger et al., 1989; Rivers & Volkert, 2023; Shinevar et al., 2021). Within published estimates, there is a consensus that the high-grade metamorphic rocks slowly cooled during the early- to mid-Tonian Period. Subsequently, the Adirondack Highlands region experienced a mild thermal history with minimal reheating, with the only magmatic activity being the intrusion of Neoproterozoic mafic dikes (such as the 9 cm dike MA11; Figure S9 in Supporting Information S1). It has been interpreted that the magmatism was associated with the opening of the Iapetus Ocean that initiated in the late Neoproterozoic (e.g., Macdonald et al., 2023). Our positive paleomagnetic baked contact test results show that heating associated with dike intrusions was limited to sub-meter scale and did not result in pervasive remagnetization of the Marcy Massif (Figure S9 in Supporting Information S1). The occurrence of Cambrian marine sedimentary rocks that unconformably overly Grenville metamorphic rocks around the Adirondack Highlands (Figure 2) indicate that the region was at or near Earth's surface at that time (ca. 510 Ma). Based on regional stratigraphic records, it has been interpreted that the most prominent stage of burial in the region occurred in the Devonian during the Acadian orogeny. The total sedimentary wedge thickens from ~2 km in western New York to ~7 km in eastern New York (Rickard & Fisher, 1975). Fluid inclusion data, index minerals, conodont alteration index data, and fission track and (U-Th)/He thermochronology data from Marcy Massif and nearby Paleozoic sedimentary rocks have consistently shown that the Adirondack Highlands was not significantly heated (<300°C) despite Paleozoic Appalachian orogenesis and the passage of the Mesozoic Great

Meteor hotspot track under the region (e.g., Allaz et al., 2013; Collins-Waite, 1987; Epstein et al., 1976; Montario & Garver, 2009; Roden-Tice & Tice, 2005; Taylor & Fitzgerald, 2011; Weary et al., 2001).

Our Marcy anorthosite rutile and apatite cooling ages provide an opportunity to evaluate previous thermal history models for the region through forward modeling. To make accurate predictions of the rutile and apatite dates, complete thermal histories are needed that start from the last time when the grains' U-Pb systems were fully open and end at the present day. Previous metamorphic petrology and geochronology studies have suggested that the Marcy Massif area reached at least ∼850°C ca. 1050 Ma during the Ottawan orogenic phase (e.g., Alcock et al., 2004; Spear & Markussen, 1997). Our zircon, garnet, and titanite U-Pb ID-TIMS data show that ∼650°C–800°C, protracted metamorphism happened ca. 1050 to 996 Ma (Figure 3c and Figures S2, S3, S5 in Supporting Information S1). Prolonged heating at such temperatures would have resulted in no retention of radiogenic Pb in rutile and apatite during Grenville peak metamorphism (Cherniak, 2000; Cherniak et al., 1991). Therefore, a reasonable starting condition for the forward modeling would be 1050–1000 Ma with an allowable temperature range of ∼650–800°C.

Mezger et al. (1991) used U-Pb and Ar geochronology data to qualitatively infer monotonic cooling histories with an exponential decay trajectory for the central and southern Adirondack areas between ca. 1050–900 Ma through a temperature range of ∼700°C–375°C (Figures 4a and 4b). Because those thermal history models are not presented in a functional form or tabulated time-temperature values in the original study, we digitized the curves, and applied an exponential fit to the thermal history curves and extrapolate them to be between 1050 Ma and present day in order to perform forward modeling. The predicted U-Pb ages for our rutile and apatite grains modeled using the Mezger et al. (1991) cooling histories are ∼100 Myr older than the observed dates (Figure 4c). This mismatch indicates that the proposed exhumation history has the region cooling through the closure temperatures too early. A similar mismatch with older predicted dates than the data is seen when the cooling history of Dahl et al. (2004) is used (Figure S10 in Supporting Information S1). Heizler and Harrison (1998) proposed a continuous thermal history for the Adirondack Highlands since ca. 950 Ma. Integrating geologic evidence and forward modeling based on $^{40}Ar/^{39}Ar$ geochronology data, that study estimated that the region might have experienced reheating up to 275–350°C at ca. 700, 470–450 and 300 Ma (Figure 4a). It was interpreted that the Tonian reheating was associated with the break up of supercontinent Rodinia, and the Paleozoic reheating events were due to fluid flow and sedimentary burial associated with Appalachian orogenesis. The predicted rutile and apatite dates for this thermal history are still distinct and older than the observed values (Figure S10 in Supporting Information S1).

We compiled the existing $^{40}Ar/^{39}Ar$ hornblende dates from the Adirondack Highlands from published literature and show them in Figures 4a and 4b. They have a peculiarly large spread between 1004 and 906 Ma. It has been observed elsewhere in the Grenville Province that hornblende and biotite in close proximity often yield wide spreads in $^{40}Ar/^{39}Ar$ ages with the oldest ones tens of millions of years older than the youngest (Dallmeyer, 1987; Dallmeyer & Rivers, 1983; Reynolds et al., 1995). There are a number of potential explanations for these issues with one hypothesis being the presence of excess argon associated with reheating events that led to the diffusion of argon liberated from adjacent lithologies (Dallmeyer & Rivers, 1983). A critical limitation of the $^{40}Ar/^{39}Ar$ approach as applied to the Grenville orogen is that previous work did not report grain size information, limiting evaluation of whether the data are consistent with volume diffusive behavior.

To explore plausible thermal histories that are compatible with our rutile and apatite U-Pb dates, we can leverage our paired grain size-age data and conduct probabilistic inversions. Given that it is the Grenvillian peak metamorphism and the following cooling that caused the most significant Pb loss in the grains, one approach is to invert for a parameterized exponential decay function such as the one approximated in the models of Mezger et al. (1991). In Figure S11 in Supporting Information S1, we show thermal history paths based on a Markov Chain Monte Carlo inversion following this functional form along with the corresponding predicted dates for our rutile and apatite. In order to acknowledge uncertainties associated with the timing and temperature of the start of Pb retention in rutile, we treat the initial timing of the thermal history to be constrained between 1050 Ma and 996 Ma, with a corresponding initial temperature condition constrained between 800°C and 650°C. The detailed inversion model framework is presented in the Supporting Information. Overall, our inverted time-temperature paths predict rutile and apatite U-Pb dates that match with the observed dates much better than previous thermal history models (Figure S11 in Supporting Information S1). The inverted paths have slow cooling rates (∼1–2°C/Myr) from the start of exponential cooling to ca. 800 Ma. As a result, the grains cooled slowly and experienced a protracted interval of diffusive Pb loss.

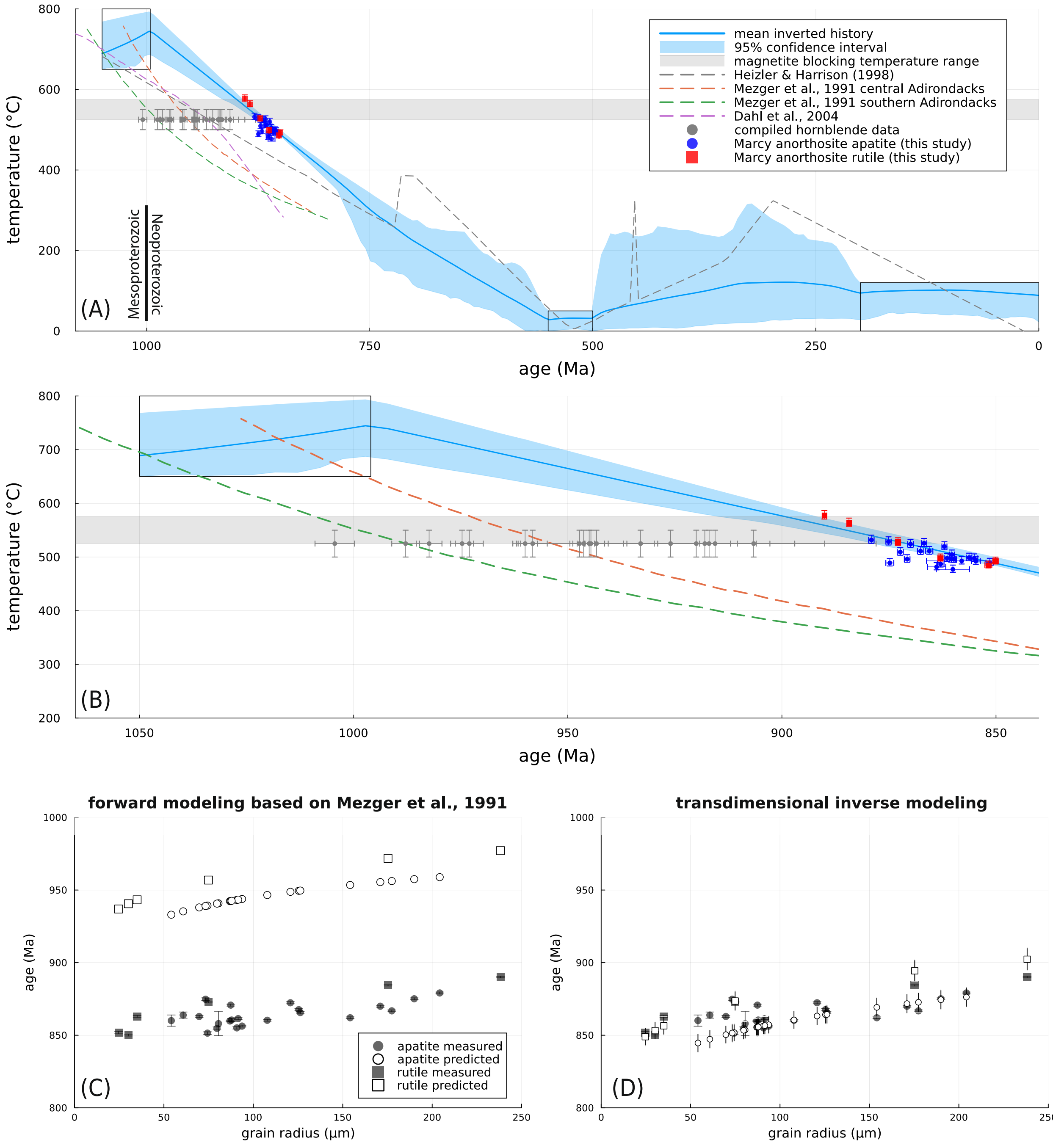

Figure 4. Thermal history modeling results for the Marcy Massif showing protracted Grenvillian metamorphism and slow Neoproterozoic cooling. (a) Our thermal history inversion results are shown along with previously proposed Neoproterozoic cooling histories (Dahl et al., 2004; Heizler & Harrison, 1998; Mezger et al., 1991), a compilation of previously developed $^{40}Ar/^{39}Ar$ hornblende geochronology data (Heizler & Harrison, 1998; Onstott & Peacock, 1987; Streepey et al., 2004) (all ages shown with 2σ), and our rutile and apatite individual grain ID-TIMS dates along with estimated closure temperatures. The closure temperatures and associated uncertainties are calculated following the theory of Dodson (1973) using a mean cooling rate of 2°C/Myr with 1°C/Myr and 3°C/Myr as the lower and upper bounds for the cooling rate. While visualizing the closure temperatures this way is illustrative, it is an oversimplification given that actual thermal history paths need not follow constant cooling (which is captured in the inversion framework). The black boxes are time-temperature constraint boxes based on zircon, garnet, and titanite data from this study, previous low-temperature thermochronology data, and geological constraints described in the text. (b) A zoom-in view of the thermal histories shown in panel (a) highlighting our data and inversion results that revise the Tonian cooling history of the Marcy Massif to be much younger than previously proposed. (c) Forward modeling results based on the cooling history for the central Adirondack Highlands proposed by Mezger et al. (1991). There is a significant mismatch between the predicted ages for rutile and apatite and observed dates. (d) Predicted rutile and apatite ages based on our transdimensional thermal history inversion compared to observed dates. The predicted values are in much better agreement with observations than forward modeling results based on all previous thermal history models (Figure S10 in Supporting Information S1).

10.1029/2025TC009333

An alternative approach to the inverse modeling is to directly search the time-temperature paths without imposing a functional form. This method allows there to be thermal histories that can include multiple cooling, plateau, or reheating phases. A unique advantage of such models is that they can include the number of time-temperature nodes as an unknown variable that is inverted for alongside the time-temperature values of the nodes. Additionally, this approach allows geological constraints to be incorporated into the inverse modeling as discrete time-temperature bounds. Implementations of such transdimensional inversion frameworks have been adopted as a routine approach in low-temperature thermochronology research (e.g., Gallagher, 2012). In these frameworks, a dimension represents a class of thermal histories with the same total number of time-temperature nodes, and the transdimensional algorithm allows the inversion model to treat the number of nodes as an inverted parameter that alter during inversion iterations. We develop such an inversion with the following constraints: zircon, garnet, and titanite U-Pb geochronology data constrain that Marcy Massif experienced ∼800°C–650°C metamorphism ca. 1050–996 Ma; geologic observations constrain that the Adirondack Highlands exhumed to the near surface ca. 550–500 Ma and were covered by Paleozoic sedimentary rocks (Rickard & Fisher, 1975; Selleck, 1980); previous thermochronology data constrain that the Adirondack Highlands was below ∼120°C at ca. 200–150 Ma and it is at the surface today (Figure 4a; Amidon et al., 2022; Roden-Tice & Tice, 2005; Taylor & Fitzgerald, 2011).

The resulting time-temperature paths show consistent cooling through ca. 1000–550 Ma, possible moderate reheating at relatively mild temperatures throughout the Paleozoic, and exhumation through the Mesozoic to today (Figure 4a). Overall, the predicted rutile and apatite dates from the inverted time-temperature paths match well with the observed dates (Figure 4d). The inverted paths reveal quasi-linear cooling trajectories throughout the Neoproterozoic. In the Paleozoic, where the inversion model setup did not include any prior information on the existence and thickness of the Paleozoic sedimentary cover in the Adirondack Highlands, the inverted results indicate that the rutile and apatite dates allow a reheating history up to mild temperatures (∼50–375°C), similar to the estimate of Heizler and Harrison (1998). These results are consistent with geologic evidence of there being a few kilometers of sedimentary burial associated with Appalachian orogenesis (Fisher, 1977; Rickard & Fisher, 1975). However, the large 95% credible interval of the thermal histories through this time indicates that the rutile and apatite U-Pb thermochronology from the Grenville basement rocks has limited resolution for reconstructing the Phanerozoic thermal history. Thermochronometers with lower closure temperatures are more suitable for precise and accurate Paleozoic burial reconstructions. Additional support that the post-Grenville reheating events in the Marcy region would have had low temperatures comes from our paleomagnetic data of MA11 and dike GD1, which show no secondary remanence components other than the present-day local field component (Figure S9 in Supporting Information S1). We interpret the transdimensional inversion results to accurately reconstruct the late Mesoproterozoic to Neoproterozoic thermal history of the Marcy Massif region.

4.4. Implications for the Paleogeography of Supercontinent Rodinia

The assembly of supercontinent Rodinia is a major event in the late Proterozoic Eon. It followed the closure of the Unimos Ocean as Laurentia rapidly traveled toward the equator, culminating in the continental collision of the ca. 1090–980 Ma Grenvillian orogeny (Hoffman, 1988; Swanson-Hysell et al., 2023). Improved chronostratigraphic constraints and paleomagnetic data from sedimentary rocks of Laurentia's interior have resulted in a ca. 1045 Ma paleomagnetic pole for the Freda Formation (Fuentes et al., 2025) and a ca. 990 Ma pole for the Jacobsville Formation (Zhang, Hodgin, et al., 2024; Figure 1a). Together with the well-dated Keweenawan Track (Swanson-Hysell et al., 2019), these data constrain that Laurentia which had been moving toward the equator at rates exceeding 20 cm/yr ca. 1110–1080 Ma (Rose et al., 2022; Swanson-Hysell et al., 2019), slowed to latitudinal drift rates of ∼2 cm/yr ca. 1080–1050 Ma, and then to ∼1 cm/yr ca. 1050–990 Ma (Fuentes et al., 2025; Zhang, Anderson, et al., 2024; Figure 5). These data are consistent with Grenvillian continent-continent collision resulting in a major plate slowdown with slow motion continuing through the Ottawan and Rigolet phases of the Grenvillian orogeny (Cannon, 1994; Hodgin et al., 2022, 2024).

The metamorphic rocks of the Grenville province are a rich paleomagnetic archive that can also be used to constrain the paleogeography of Rodinia. Figure 1a shows a selection of previously developed paleomagnetic poles of the Grenville Loop which consistently plot near Australia in present-day coordinates (Halls, 2015). Those poles form arc distances of ∼50° from poles at the end of the ca. 1110 to 1070 Ma Keweenawan Track. Given that paleomagnetic field tests constrain the Jacobsville pole to be a primary detrital remanent magnetization (Zhang, Hodgin, et al., 2024), and that its age is chronostratigraphically well-constrained (Hodgin et al., 2022), we consider it to be a reliable representation of the position of Laurentia ca. 990 Ma. Solutions for the discrepancy

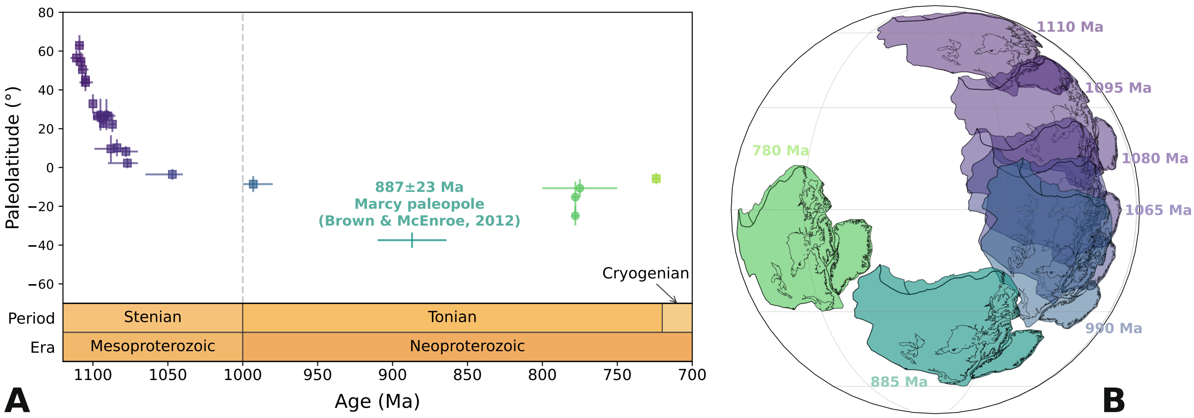

Figure 5. Paleogeography summary for Laurentia from the late Stenian Period of the Mesoproterozoic through the Tonian Period of the Neoproterozoic. (a) Paleolatitude progression for Duluth, Minnesota, USA (46.78°N, 92.10°W) calculated from paleomagnetic poles. Based on the geochronology data and transdimensional thermal inversion results in this study, the Marcy Massif anorthosite paleopole developed by L. Brown and McEnroe (2012) is dated to be 887 ± 23 Ma—providing a mid-Tonian constraint on Rodinia paleogeography. (b) Paleogeographic reconstruction for Laurentia ca. 1110–780 Ma. Following rapid equatorward plate tectonic motion in the late Mesoproterozoic, the onset of the Grenvillian orogenesis caused a significant slowdown in Laurentia's plate speed in the Neoproterozoic. The assembled supercontinent Rodinia then traveled into the southern hemisphere, and eventually back up again toward the equator leading up to its breakup in the late Tonian. Data are compiled from Evans et al. (2021) with updates from Zhang, Anderson, et al. (2024), Fuentes et al. (2025), and Ding et al. (2025).

between the Jacobsville pole and the Grenville poles that call upon separation between Laurentia and the Grenville Province at the time (e.g., Halls, 2015) are not feasible given how late this timing is within the overall history of orogenesis. The Grenville poles must represent Laurentia's paleogeographic position, but at what time?

Integrating the geochronological, thermochronological, and paleomagnetic data from the Marcy Massif, we quantitatively constrain the age and the associated uncertainties of the pole position developed from the Marcy anorthositic rocks. Based on thermal demagnetization data, L. Brown and McEnroe (2012) interpreted that near-stoichiometric low-titanium magnetite in Marcy anorthositic rocks acquired magnetic remanence as the rocks cooled through ∼575–525°C. Projecting a nominal magnetic remanence blocking temperature of 570°C onto the central Adirondack Highlands thermal history of Mezger et al. (1991), they estimated an age of ca. 970 Ma for the Marcy anorthosite paleomagnetic pole position. Our transdimensional thermal history inversion results show that the Marcy Massif cooled to ∼570°C at 896^{+14}_{-8} Ma, and cooled to 525°C at 870^{+8}_{-6} Ma (95% CI). The majority of the characteristic remanence in the rocks unblock at the ∼550°C step that L. Brown and McEnroe (2012) applied following a ∼575°C step. According to our inverted thermal histories, the Marcy Massif cooled to 550°C at 885^{+9}_{-7} Ma. Additional uncertainties associated with the timing of magnetic remanence acquisition come from the potential cooling rate effect on lowering the natural magnetic remanence blocking temperatures in the anorthositic rocks (Dodson & McClelland-Brown, 1980; Halgedahl et al., 1980). Applying single domain theory using the slow ∼2°C/Myr cooling rate would result in the ∼575°C–550°C unblocking temperatures corresponding to natural remanence blocking temperatures of ∼570°C to 525°C. While natural blocking temperature to laboratory unblocking temperature relationships are not well-constrained for vortex-state grains, available data indicate that they can be reciprocal (Almeida et al., 2016). Any bias toward lower blocking temperatures relative to laboratory unblocking would push age estimates to be younger. We consider a conservative estimate of the timing of titanomagnetite remanence acquisition to encompass age uncertainty associated with cooling to ∼570°C to ∼525°C at 910–864 Ma. A succinct presentation of the age and uncertainty of the pole is that it is 887 ± 23 Ma (Figure 5).

Overall, our thermal history reconstructions recalibrate the Marcy anorthosite paleomagnetic pole to be ∼85 Ma younger than previously considered. As a result, a straightforward tectonic model for the development of the paleogeography of Laurentia that satisfies both the ca. 990 Ma Jacobsville Formation pole and the Marcy anorthosite pole is that the continent slowly moved from a low-latitude position ca. 990 Ma to southern high latitudes ca. 885 Ma (Figure 5b). This slow plate motion is geodynamically consistent with the collisional Grenvillian orogeny and the final assembly of the Rodinia supercontinent in the early Neoproterozoic. As a result, our updated interpretation of Laurentia's Tonian apparent polar wander path does not require there to be large-scale, rapid true polar wander to link the Mesoproterozoic Keweenawan Track to the Neoproterozoic Grenville Loop (Figure 5).

Recent geochronology data hint that other paleomagnetic poles in the Grenville Loop might also have ages significantly postdating Grenvillian orogenesis. For example, Paul et al. (2021) obtained a 923 ± 14 Ma (2σ analytical) apatite U-Pb age in Wilberforce, Ontario that could indicate that magnetite magnetizations in that region are of a similar age. Conversely, we consider it unlikely that intrusive rocks in the Haliburton Highlands acquired their magnetization while Grenvillian peak metamorphism was ongoing as is implied by the age assignment of ca. 1015 Ma that is applied in pole compilations (Figure 1a; e.g., Evans et al., 2021; Li et al., 2008). Developing more detailed paleomagnetic data paired with geochronology data, including U-Pb apatite thermochronology, can better calibrate the paleopoles of the Grenville Loop and the motion of Laurentia in reconstructions of the configuration and position of Rodinia.

5. Conclusion

Our new suite of zircon, garnet, titanite, rutile, and apatite geochronology and geochemistry data and the quantitative reconstruction of the thermal history of the Marcy Massif recalibrate the post-Grenville exhumation history of the Adirondack Highlands and global paleogeography of Laurentia in the Neoproterozoic Era. By combining U-Pb geochronology and thermochronology data and probabilistic inversion modeling, we show that the Marcy Massif experienced complex and protracted high-grade metamorphism during both the ca. 1090–1020 Ma Ottawan orogenic phase and the ca. 1010–980 Ma Rigolet phase, followed by slow cooling through the Neoproterozoic Era. By pairing the new thermal history data with paleomagnetic data, we reinterpret the Grenville Loop to represent the configuration of Laurentia and supercontinent Rodinia well after Grenvillian orogenesis. Global paleogeography from early- to mid-Tonian most likely featured a slowly drifting supercontinent Rodinia whose center moved from equatorial latitudes ca. 990 Ma to southern high latitudes ca. 887 Ma. Other paleomagnetic poles developed from high-grade metamorphic rocks need to be paired with quantitatively constrained thermal histories for accurate paleogeography reconstructions.

Conflict of Interest

The authors declare no conflicts of interest relevant to this study.

Availability Statement

Data sets and data analysis code are available within the GitHub repository (https://github.com/Swanson-Hysell-Group/Adirondack_mountains) that has been archived on Zenodo (http://doi.org/10.5281/zenodo.18943207). The paleomagnetic data are available in the Magnetics Information Consortium (MagIC) database (http://doi.org/10.7288/V4/MAGIC/20549).

Acknowledgments
Project research was funded by NSF CAREER Grant EAR-1847277 to N.L.S.-H., an H2H8 Association Graduate Research Grant to Y.Z., an AGeS-Grad Grant to Y.Z., and an Esper S. Larsen Jr. Research Fund grant to N.L.S.-H and E.B. H. The AGeS-Grad program was supported by the National Science Foundation under Grant EAR-2218547 and EAR-2218544. Funding for the analytical infrastructure of the IGL used in this study was provided by NSF Grants EAR-1735889, EAR-1920336 and EAR-1337887. Any opinions, findings, and conclusions or recommendations expressed in this material are those of the author(s) and do not necessarily reflect the views of the National Science Foundation. Y.Z. thanks Facundo Sapienza for discussions of the inverse modeling. We thank Matthew Kohn for kindly providing the Willsboro-Lewis garnet samples. We thank Laurie Brown for providing paleomagnetic sampling localities in her 2012 study. This is IRM Contribution 2601.

References

Alcock, J., Isachsen, C., Livi, K., & Muller, P. (2004). Unraveling growth history of zircon in anatectites from the northeast Adirondack Highlands, New York: Constraints on pressure-temperature-time paths. In *Memoir 197: Proterozoic tectonic evolution of the Grenville orogen in North America* (pp. 267–284). Geological Society of America. https://doi.org/10.1130/0-8137-1197-5.267

Aleinikoff, J. N., Walsh, G. J., & McAleer, R. J. (2021). New interpretations of the ages and origins of the Hawkeye Granite Gneiss and Lyon Mountain Granite Gneiss, Adirondack Mountains, NY: Implications for the nature and timing of Mesoproterozoic plutonism, metamorphism, and deformation. *Precambrian Research*, *358*, 106112. https://doi.org/10.1016/j.precamres.2021.106112

Allaz, J., Selleck, B., Williams, M. L., & Jercinovic, M. J. (2013). Microprobe analysis and dating of monazite from the Potsdam Formation, New York: A progressive record of chemical reaction and fluid interaction†. *American Mineralogist*, *98*(7), 1106–1119. https://doi.org/10.2138/am.2013.4304

Almeida, T. P., Muxworthy, A. R., Kovács, A., Williams, W., Brown, P. D., & Dunin-Borkowski, R. E. (2016). Direct visualization of the thermomagnetic behavior of pseudo–single-domain magnetite particles. *Science Advances*, *2*(4), e1501801. https://doi.org/10.1126/sciadv.1501801

Amidon, W. H., Kylander-Clark, A. R. C., Barr, M. N., Graf, S. F. I., & West, D. P. (2022). Pace of passive margin tectonism revealed by U-Pb dating of fracture-filling calcite. *Nature Communications*, *13*(1), 1953. https://doi.org/10.1038/s41467-022-29680-z

Beno, C. J., Lackey, J. S., Schmitz, M. D., Bowman, J. R., Stearns, M. A., Bartley, J. M., & Fernandez, D. P. (2024). Assessment of natural reference materials for U-Pb geochronology of grossular-andradite garnet. *Geostandards and Geoanalytical Research*, *48*(4), 909–925. https://doi.org/10.1111/ggr.12561

Berger, G. W., York, D., & Dunlop, D. J. (1979). Calibration of Grenvillian palaeopoles by 40Ar/39Ar dating. *Nature*, *277*(5691), 46–48. https://doi.org/10.1038/277046a0

Beucher, R., Brown, R. W., Roper, S., Stuart, F., & Persano, C. (2013). Natural age dispersion arising from the analysis of broken crystals: Part II. Practical application to apatite (U–Th)/He thermochronometry. *Geochimica et Cosmochimica Acta*, *120*, 395–416. https://doi.org/10.1016/j.gca.2013.05.042

Beyer, C., Dohmen, R., Rogalla, D., Becker, H.-W., Marquardt, K., Vollmer, C., et al. (2019). Lead diffusion in CaTiO3: A combined study using Rutherford backscattering and TOF-SIMS for depth profiling to reveal the role of lattice strain in diffusion processes. *American Mineralogist*, *104*(4), 557–568. https://doi.org/10.2138/am-2019-6730

Bohlen, S. R., Valley, J. W., & Essene, E. J. (1985). Metamorphism in the Adirondacks. I. Petrology, pressure and temperature. *Journal of Petrology*, *26*(4), 971–992. https://doi.org/10.1093/petrology/26.4.971

Brown, L., & McEnroe, S. (2012). Paleomagnetism and magnetic mineralogy of Grenville metamorphic and igneous rocks, Adirondack Highlands, USA. *Precambrian Research*, *212–213*, 57–74. https://doi.org/10.1016/j.precamres.2012.04.012

Brown, R. W., Beucher, R., Roper, S., Persano, C., Stuart, F., & Fitzgerald, P. (2013). Natural age dispersion arising from the analysis of broken crystals. Part I: Theoretical basis and implications for the apatite (U–Th)/He thermochronometer. *Geochimica et Cosmochimica Acta*, *122*, 478–497. https://doi.org/10.1016/j.gca.2013.05.041

Buchanan, A. L. (2015). *Timing and evolution of metasomatic alteration and mineralization in the Lyon Mountain Granite and related iron oxide apatite (IOA) ores; constraints from apatite and titanite U-Pb geochronology, Sm-Nd isotopes and trace-elements* (Unpublished master's thesis). Memorial University of Newfoundland.

Cannon, W. F. (1994). Closing of the Midcontinent Rift—A far-field effect of Grenvillian compression. *Geology*, *22*(2), 155. https://doi.org/10.1130/0091-7613(1994)022⟨0155:cotmra⟩2.3.co;2

Cannon, W. F., Peterman, Z. E., & Sims, P. K. (1993). Crustal-scale thrusting and origin of the Montreal River Monocline-A 35-km-thick cross section of the Midcontinent Rift in northern Michigan and Wisconsin. *Tectonics*, *12*(3), 728–744. https://doi.org/10.1029/93tc00204

Cherniak, D. J. (1993). Lead diffusion in titanite and preliminary results on the effects of radiation damage on Pb transport. *Chemical Geology*, *110*(1–3), 177–194. https://doi.org/10.1016/0009-2541(93)90253-f

Cherniak, D. J. (2000). Pb diffusion in rutile. *Contributions to Mineralogy and Petrology*, *139*(2), 198–207. https://doi.org/10.1007/pl00007671

Cherniak, D. J. (2006). Zr diffusion in titanite. *Contributions to Mineralogy and Petrology*, *152*(5), 639–647. https://doi.org/10.1007/s00410-006-0133-0

Cherniak, D. J., Hanchar, J. M., & Watson, E. B. (1997). Diffusion of tetravalent cations in zircon. *Contributions to Mineralogy and Petrology*, *127*(4), 383–390. https://doi.org/10.1007/s004100050287

Cherniak, D. J., Lanford, W., & Ryerson, F. (1991). Lead diffusion in apatite and zircon using ion implantation and Rutherford Backscattering techniques. *Geochimica et Cosmochimica Acta*, *55*(6), 1663–1673. https://doi.org/10.1016/0016-7037(91)90137-t

Cherniak, D. J., & Watson, E. (2001). Pb diffusion in zircon. *Chemical Geology*, *172*(1–2), 5–24. https://doi.org/10.1016/s0009-2541(00)00233-3

Chiarenzelli, J., Regan, S., Peck, W. H., Selleck, B. W., Cousens, B., Baird, G. B., & Shrady, C. H. (2010). Shawinigan arc magmatism in the Adirondack Lowlands as a consequence of closure of the Trans-Adirondack backarc basin. *Geosphere*, *6*(6), 900–916. https://doi.org/10.1130/ges00576.1

Clechenko, C. C., & Valley, J. W. (2003). Oscillatory zoning in garnet from the Willsboro Wollastonite Skarn, Adirondack Mts, New York: A record of shallow hydrothermal processes preserved in a granulite facies terrane. *Journal of Metamorphic Geology*, *21*(8), 771–784. https://doi.org/10.1046/j.1525-1314.2003.00478.x

Collins-Waite, D. (1987). *Diagenesis of the Cambro-Ordovician Beekmantown Group: A petrographic and fluid inclusion study* (Unpublished doctoral dissertation). Colgate University.

Corfu, F., & Stone, D. (1998). The significance of titanite and apatite U-Pb ages: Constraints for the post-magmatic thermal-hydrothermal evolution of a batholithic complex, Berens River area, northwestern Superior Province, Canada. *Geochimica et Cosmochimica Acta*, *62*(17), 2979–2995. https://doi.org/10.1016/S0016-7037(98)00225-7

Cosca, M. A., Sutter, J. F., & Essene, E. J. (1991). Cooling and inferred uplift/erosion history of the Grenville orogen, Ontario: Constraints from 40Ar/39Ar thermochronology. *Tectonics*, *10*(5), 959–977. https://doi.org/10.1029/91tc00859

Dahl, P. S., Pomfrey, M. E., & Foland, K. A. (2004). Slow cooling and apparent tilting of the Adirondack Lowlands, Grenville Province, New York, based on 40Ar/39Ar ages. In *Memoir 197: Proterozoic tectonic evolution of the Grenville orogen in North America* (pp. 299–323). Geological Society of America. https://doi.org/10.1130/0-8137-1197-5.299

Dallmeyer, R. D. (1987). 40Ar/39Ar mineral age record of variably superimposed Proterozoic tectonothermal events in the Grenville orogen, central Labrador. *Canadian Journal of Earth Sciences*, *24*(2), 314–333. https://doi.org/10.1139/e87-033

Dallmeyer, R. D., & Rivers, T. (1983). Recognition of extraneous argon components through incremental-release analysis of biotite and hornblende across the Grenvillian metamorphic gradient in southwestern Labrador. *Geochimica et Cosmochimica Acta*, *47*(3), 413–428. https://doi.org/10.1016/0016-7037(83)90264-8

Dewolf, C. P., Zeissler, C. J., Halliday, A. N., Mezger, K., & Essene, E. J. (1996). The role of inclusions in U-Pb and Sm-Nd garnet geochronology: Stepwise dissolution experiments and trace uranium mapping by fission track analysis. *Geochimica et Cosmochimica Acta*, *60*(1), 121–134. https://doi.org/10.1016/0016-7037(95)00367-3

Dicken, C. L., Nicholson, S. W., Horton, J. D., Kinney, S. A., Gunther, G., Foose, M. P., & Mueller, J. A. L. (2005). *Preliminary integrated geologic map databases for the United States: Delaware, Maryland, New York, Pennsylvania, and Virginia* (Technical Report). U.S. Geological Survey/U.S. Geological Survey. https://doi.org/10.3133/ofr20051325

Ding, J., Evans, D. A. D., Kilian, T., Mitchell, R. N., Gong, Z., Chamberlain, K., et al. (2025). Local rotations biasing supercontinental configurations: Revisiting a key ca. 780 Ma paleomagnetic pole for Laurentia and Rodinia. *Journal of Geophysical Research: Solid Earth*, *130*(11), e2025JB031762. https://doi.org/10.1029/2025JB031762

Dodson, M. H. (1973). Closure temperature in cooling geochronological and petrological systems. *Contributions to Mineralogy and Petrology*, *40*(3), 259–274. https://doi.org/10.1007/bf00373790

Dodson, M. H., & McClelland-Brown, E. (1980). Magnetic blocking temperatures of single-domain grains during slow cooling. *Journal of Geophysical Research*, *85*(B5), 2625–2637. https://doi.org/10.1029/jb085ib05p02625

Dunlop, D., & Özdemir, Ö. (2015). Magnetizations in rocks and minerals. In *Treatise on geophysics* (pp. 255–308). Elsevier. https://doi.org/10.1016/b978-0-444-53802-4.00102-0

Epstein, A. G., Epstein, J. B., & Harris, L. D. (1976). *Conodont color alteration: An index to organic metamorphism*. US Government Printing Office.

Evans, D. A. D. (2003). True polar wander and supercontinents. *Tectonophysics*, *362*(1–4), 303–320. https://doi.org/10.1016/s0040-1951(02)000642-x

Evans, D. A. D., Pesonen, L. J., Eglington, B. M., Elming, S.-Å., Gong, Z., Li, Z.-X., et al. (2021). An expanding list of reliable paleomagnetic poles for Precambrian tectonic reconstructions. In *Ancient supercontinents and the paleogeography of Earth* (pp. 605–639). Elsevier. https://doi.org/10.1016/b978-0-12-818533-9.00007-2

Fairchild, L. M., Swanson-Hysell, N. L., Ramezani, J., Sprain, C. J., & Bowring, S. A. (2017). The end of Midcontinent Rift magmatism and the paleogeography of Laurentia. *Lithosphere*, *9*(1), 117–133. https://doi.org/10.1130/l580.1

Ferry, J. M., & Watson, E. B. (2007). New thermodynamic models and revised calibrations for the Ti-in-zircon and Zr-in-rutile thermometers. *Contributions to Mineralogy and Petrology*, *154*(4), 429–437. https://doi.org/10.1007/s00410-007-0201-0

Fisher, D. W. (1977). *Correlation of the Hadrynian, Cambrian and Ordovician rocks in New York state* (Technical Report). New York State Museum.

Fuentes, A. J., Fairchild, L. M., Hodgin, E. B., Alemu, T., & Swanson-Hysell, N. (2025). Termination of Laurentia's rapid plate motion at the start of the Grenvillian orogeny. *Journal of Geophysical Research: Solid Earth*, *130*(8), e2025JB031794. https://doi.org/10.1029/2025JB031794

Gallagher, K. (2012). Transdimensional inverse thermal history modeling for quantitative thermochronology. *Journal of Geophysical Research*, *117*(B2). https://doi.org/10.1029/2011jb008825

Gao, X.-Y., Zheng, Y.-F., Chen, Y.-X., & Guo, J. (2012). Geochemical and U–Pb age constraints on the occurrence of polygenetic titanites in UHP metagranite in the Dabie orogen. *Lithos*, *136–139*, 93–108. https://doi.org/10.1016/j.lithos.2011.03.020

Garber, J. M., Hacker, B. R., Kylander-Clark, A. R. C., Stearns, M., & Seward, G. (2017). Controls on trace element uptake in metamorphic titanite: Implications for petrochronology. *Journal of Petrology*, *58*(6), 1031–1057. https://doi.org/10.1093/petrology/egx046

Halgedahl, S. L., Day, R., & Fuller, M. (1980). The effect of cooling rate on the intensity of weak-field TRM in single-domain magnetite. *Journal of Geophysical Research*, *85*(B7), 3690–3698. https://doi.org/10.1029/jb085ib07p03690

Halls, H. C. (2015). Paleomagnetic evidence for ~4000 km of crustal shortening across the 1 Ga Grenville orogen of North America. *Geology*, G37188.1. https://doi.org/10.1130/g37188.1

Halls, H. C., Lovette, A., Hamilton, M., & Söderlund, U. (2015). A paleomagnetic and U–Pb geochronology study of the western end of the Grenville dyke swarm: Rapid changes in paleomagnetic field direction at ca. 585 Ma related to polarity reversals? *Precambrian Research*, *257*, 137–166. https://doi.org/10.1016/j.precamres.2014.11.029

Hargraves, R. B., & Burt, D. M. (1967). Paleomagnetism of the Allard Lake anorthosite suite. *Canadian Journal of Earth Sciences*, *4*(3), 357–369. https://doi.org/10.1139/e67-018

Harlan, S. S., Heaman, L., LeCheminant, A. N., & Premo, W. R. (2003). Gunbarrel mafic magmatic event: A key 780 Ma time marker for Rodinia plate reconstructions. *Geology*, *31*(12), 1053. https://doi.org/10.1130/g19944.1

Harrison, R. J. (2006). Microstructure and magnetism in the ilmenite-hematite solid solution: A Monte Carlo simulation study. *American Mineralogist*, *91*(7), 1006–1024. https://doi.org/10.2138/am.2006.2008

Hayden, L. A., Watson, E. B., & Wark, D. A. (2007). A thermobarometer for sphene (titanite). *Contributions to Mineralogy and Petrology*, *155*(4), 529–540. https://doi.org/10.1007/s00410-007-0256-y

Heizler, M. T., & Harrison, T. M. (1998). The thermal history of the New York basement determined from 40Ar/39Ar K-feldspar studies. *Journal of Geophysical Research*, *103*(B12), 29795–29814. https://doi.org/10.1029/98jb02837

Heumann, M. J., Bickford, M., Hill, B. M., McLelland, J. M., Selleck, B. W., & Jercinovic, M. J. (2006). Timing of anatexis in metapelites from the Adirondack lowlands and southern highlands: A manifestation of the Shawinigan orogeny and subsequent anorthosite-mangerite-charnockite-granite magmatism. *Geological Society of America Bulletin*, *118*(11–12), 1283–1298. https://doi.org/10.1130/b25927.1

Hodgin, E. B., Swanson-Hysell, N. L., DeGraff, J. M., Kylander-Clark, A. R., Schmitz, M. D., Turner, A. C., et al. (2022). Final inversion of the Midcontinent Rift during the Rigolet Phase of the Grenvillian Orogeny. *Geology*, *50*(5), 547–551. https://doi.org/10.1130/g49439.1

Hodgin, E. B., Swanson-Hysell, N. L., Kylander-Clark, A. R. C., Turner, A. C., Stolper, D. A., Ibarra, D. E., et al. (2024). One billion years of stability in the North American midcontinent following two-stage Grenvillian structural inversion. *Tectonics*, *43*(9), e2024TC008415. https://doi.org/10.1029/2024tc008415

Hoffman, P. F. (1988). United plates of America, the birth of a craton: Early Proterozoic assembly and growth of Laurentia. *Annual Review of Earth and Planetary Sciences*, *16*(1), 543–603. https://doi.org/10.1146/annurev.ea.16.050188.002551

Hoffman, P. F. (1991). Did the breakout of Laurentia turn Gondwanaland inside-out? *Science*, *252*(5011), 1409–1412. https://doi.org/10.1126/science.252.5011.1409

Hynes, A., & Rivers, T. (2010). Protracted continental collision – Evidence from the Grenville orogen. *Canadian Journal of Earth Sciences*, *47*(5), 591–620. https://doi.org/10.1139/e10-003

Hyodo, H., & Dunlop, D. J. (1993). Effect of anisotropy on the paleomagnetic contact test for a Grenville Dike. *Journal of Geophysical Research*, *98*(B5), 7997–8017. https://doi.org/10.1029/92jb02915

Indares, A. (1993). Eclogitized gabbros from the eastern Grenville Province: Textures, metamorphic context, and implications. *Canadian Journal of Earth Sciences*, *30*(1), 159–173. https://doi.org/10.1139/e93-015

Indares, A. (1995). Metamorphic interpretation of high-pressure-temperature metapelites with preserved growth zoning in garnet, eastern Grenville Province, Canadian Shield. *Journal of Metamorphic Geology*, *13*(4), 475–486. https://doi.org/10.1111/j.1525-1314.1995.tb00235.x

Indares, A. (2024). The Grenville Province: Revisiting the orogenic framework and integrating recent findings. *Canadian Journal of Earth Sciences*, *62*(2), 99–118. https://doi.org/10.1139/cjes-2023-0143

Indares, A., & Dunning, G. (1997). Coronitic metagabbro and eclogite from the Grenville Province of western Quebec: Interpretation of U–Pb geochronology and metamorphism. *Canadian Journal of Earth Sciences*, *34*(7), 891–901. https://doi.org/10.1139/e17-074

Jannin, S., Gervais, F., Moukhsil, A., & Augland, L. E. (2018). Late-Grenvillian channel flow in the central Grenville Province (Manicouagan Reservoir area): New constraints from a structural and geochronological study of the Allochthon Boundary Thrust. *Journal of Structural Geology*, *115*, 132–151. https://doi.org/10.1016/j.jsg.2018.07.019

Kamo, S. L., Krogh, T. E., & Kumarapeli, P. S. (1995). Age of the Grenville dyke swarm, Ontario–Quebec: Implications for the timing of Iapetan rifting. *Canadian Journal of Earth Sciences*, *32*(3), 273–280. https://doi.org/10.1139/e95-022

Kemp, J. F. (1898). *Geology of the Lake placid region* (Technical Report). New York State Museum.

Kohn, M. J. (2020). A refined zirconium-in-rutile thermometer. *American Mineralogist*, *105*(6), 963–971. https://doi.org/10.2138/am-2020-7091

Kohn, M. J., & Corrie, S. L. (2011). Preserved Zr-temperatures and U–Pb ages in high-grade metamorphic titanite: Evidence for a static hot channel in the Himalayan orogen. *Earth and Planetary Science Letters*, *311*(1), 136–143. https://doi.org/10.1016/j.epsl.2011.09.008

Kohn, M. J., & Valley, J. W. (1998). Effects of cation substitutions in garnet and pyroxene on equilibrium oxygen isotope fractionations. *Journal of Metamorphic Geology*, *16*(5), 625–639. https://doi.org/10.1111/j.1525-1314.1998.00162.x

Krestianinov, E., Amelin, Y., Neymark, L. A., & Aleinikoff, J. N. (2021). U-Pb systematics of uranium-rich apatite from Adirondacks: Inferences about regional geological and geochemical evolution, and evaluation of apatite reference materials for in situ dating. *Chemical Geology*, *581*, 120417. https://doi.org/10.1016/j.chemgeo.2021.120417

Lambert, C., Gervais, F., Crowley, J. L., Moukhsil, A., & Kavanagh-Lepage, C. (2023). Protracted melt-present deformation during the Rigolet phase of the Grenvillian Orogeny. Insights from geochronology along the highway 117 transect through the Grenville Province in western Quebec, Canada. *Precambrian Research*, *384*, 106939. https://doi.org/10.1016/j.precamres.2022.106939

Li, Z., Bogdanova, S., Collins, A., Davidson, A., Waele, B. D., Ernst, R., et al. (2008). Assembly, configuration, and break-up history of Rodinia: A synthesis. *Precambrian Research*, *160*(1–2), 179–210. https://doi.org/10.1016/j.precamres.2007.04.021

Macdonald, F. A., Yonkee, W. A., Flowers, R. M., & Swanson-Hysell, N. L. (2023). Neoproterozoic of Laurentia. In *Laurentia: Turning points in the evolution of a continent* (pp. 331–380). Geological Society of America. https://doi.org/10.1130/2022.1220
Mackinder, A., Cousens, B. L., Ernst, R. E., & Chamberlain, K. R. (2019). Geochemical, isotopic, and U–Pb zircon study of the central and southern portions of the 780 Ma Gunbarrel Large Igneous Province in western Laurentia. *Canadian Journal of Earth Sciences*, *56*(7), 738–755. https://doi.org/10.1139/cjes-2018-0083
Martignole, J., & Reynolds, P. (1997). 40Ar/39Ar thermochronology along a western Québec transect of the Grenville Province, Canada. *Journal of Metamorphic Geology*, *15*(2), 283–296. https://doi.org/10.1111/j.1525-1314.1997.00018.x
Mattinson, J. M. (1978). Age, origin, and thermal histories of some plutonic rocks from the Salinian block of California. *Contributions to Mineralogy and Petrology*, *67*(3), 233–245. https://doi.org/10.1007/BF00381451
Mattinson, J. M. (2005). Zircon U–Pb chemical abrasion ("CA-TIMS") method: Combined annealing and multi-step partial dissolution analysis for improved precision and accuracy of zircon ages. *Chemical Geology*, *220*(1–2), 47–66. https://doi.org/10.1016/j.chemgeo.2005.03.011
McEnroe, S. A., Robinson, P., Langenhorst, F., Frandsen, C., Terry, M. P., & Ballaran, T. B. (2007). Magnetization of exsolution intergrowths of hematite and ilmenite: Mineral chemistry, phase relations, and magnetic properties of hemo-ilmenite ores with micron-to nanometer-scale lamellae from Allard Lake, Quebec. *Journal of Geophysical Research*, *112*(B10). https://doi.org/10.1029/2007jb004973
McLelland, J. M. (2016). Regional geological setting of the Adirondack Mountains, New York. *Adirondack Journal of Environmental Studies*, *21*(1), 4.
McLelland, J. M., Ashwal, L., & Moore, L. (1994). Composition and petrogenesis of oxide-apatite-rich gabbronorites associated with Proterozoic anorthosite massifs: Examples from the Adirondack Mountains, New York. *Contributions to Mineralogy and Petrology*, *116*(1–2), 225–238. https://doi.org/10.1007/bf00310702
McLelland, J. M., Bickford, M. E., Hill, B. M., Clechenko, C. C., Valley, J. W., & Hamilton, M. A. (2004). Direct dating of Adirondack massif anorthosite by U-Pb SHRIMP analysis of igneous zircon: Implications for AMCG complexes. *GSA Bulletin*, *116*(11–12), 1299–1317. https://doi.org/10.1130/b25482.1
McLelland, J. M., Chiarenzelli, J., Whitney, P., & Isachsen, Y. (1988). U-Pb zircon geochronology of the Adirondack Mountains and implications for their geologic evolution. *Geology*, *16*(10), 920. https://doi.org/10.1130/0091-7613(1988)016⟨0920:upzgot⟩2.3.co;2
McLelland, J. M., Selleck, B. W., & Bickford, M. (2010). Review of the Proterozoic evolution of the Grenville Province, its Adirondack outlier, and the Mesoproterozoic inliers of the Appalachians. In *From Rodinia to Pangea: The lithotectonic record of the Appalachian region*. Geological Society of America. https://doi.org/10.1130/2010.1206(02
McLelland, J. M., Selleck, B. W., Hamilton, M. A., & Bickford, M. E. (2010). Late-to post-tectonic setting of some major Proterozoic anorthosite-mangerite-charnokite—Granite (AMCG) suites. *The Canadian Mineralogist*, *48*(4), 729–750. https://doi.org/10.3749/canmin.48.4.729
McLelland, J. M., & Whitney, P. R. (1977). The origin of garnet in the anorthosite-charnockite suite of the Adirondacks. *Contributions to Mineralogy and Petrology*, *60*(2), 161–181. https://doi.org/10.1007/bf00372280
McWilliams, M. O., & Dunlop, D. J. (1975). Precambrian paleomagnetism: Magnetizations reset by the Grenville Orogeny. *Science*, *190*(4211), 269–272. https://doi.org/10.1126/science.190.4211.269
Metzger, E. P., Leech, M. L., Davis, M. W., Reeder, J. V., Swanson, B. A., & Waring, H. V. (2021). Ultrahigh-temperature granulite-facies metamorphism and exhumation of deep crust in a migmatite dome during late-to post- orogenic collapse and extension in the central Adirondack Highlands (New York, USA). *Geosphere*, *18*(1), 261–297. https://doi.org/10.1130/ges02318.1
Mezger, K., Hanson, G., & Bohlen, S. (1989). High-precision U-Pb ages of metamorphic rutile: Application to the cooling history of high-grade terranes. *Earth and Planetary Science Letters*, *96*(1–2), 106–118. https://doi.org/10.1016/0012-821x(89)90126-x
Mezger, K., & Krogstad, E. J. (1997). Interpretation of discordant U-Pb zircon ages: An evaluation. *Journal of Metamorphic Geology*, *15*(1), 127–140. https://doi.org/10.1111/j.1525-1314.1997.00008.x
Mezger, K., Rawnsley, C. M., Bohlen, S. R., & Hanson, G. N. (1991). U-Pb garnet, sphene, monazite, and rutile ages: Implications for the duration of high-grade metamorphism and cooling histories, Adirondack Mts., New York. *The Journal of Geology*, *99*(3), 415–428. https://doi.org/10.1086/629503
Miller, W. J., & Alling, H. L. (1918). *Geology of the Lake Placid quadrangle* (Vol. 211/212). University of the State of New York.
Milton, J. E., Hickey, K. A., Gleeson, S. A., & Friedman, R. M. (2017). New U-Pb constraints on the age of the Little Dal Basalts and Gunbarrel-related volcanism in Rodinia. *Precambrian Research*, *296*, 168–180. https://doi.org/10.1016/j.precamres.2017.04.030
Montario, M. J., & Garver, J. I. (2009). The thermal evolution of the Grenville terrane revealed through U-Pb and fission-track analysis of detrital zircon from Cambro-Ordovician quartz arenites of the Potsdam and Galway Formations. *The Journal of Geology*, *117*(6), 595–614. https://doi.org/10.1086/605778
Odlum, M. L., Levy, D. A., Stockli, D. F., Stockli, L. D., & DesOrmeau, J. W. (2022). Deformation and metasomatism recorded by single-grain apatite petrochronology. *Geology*, *50*(6), 697–703. https://doi.org/10.1130/g49809.1
Onstott, T., & Peacock, M. (1987). Argon retentivity of hornblendes: A field experiment in a slowly cooled metamorphic terrane. *Geochimica et Cosmochimica Acta*, *51*(11), 2891–2903. https://doi.org/10.1016/0016-7037(87)90365-6
Palmer, H. C., & Davis, D. W. (1987). Paleomagnetism and U-Pb geochronology of volcanic rocks from Michipicoten Island, Lake Superior, Canada: Precise calibration of the Keweenawan polar wander track. *Precambrian Research*, *37*(2), 157–171. https://doi.org/10.1016/0301-9268(87)90077-5
Paul, A. N., Spikings, R. A., & Gaynor, S. P. (2021). U-Pb ID-TIMS reference ages and initial Pb isotope compositions for Durango and Wilberforce apatites. *Chemical Geology*, *586*, 120604. https://doi.org/10.1016/j.chemgeo.2021.120604
Peck, W. H., Selleck, B. W., Regan, S. P., Howard, G. E., & Kozel, O. O. (2018). In-situ dating of metamorphism in Adirondack anorthosite. *American Mineralogist*, *103*(10), 1523–1529. https://doi.org/10.2138/am-2018-6481
Peck, W. H., Selleck, B. W., Wong, M. S., Chiarenzelli, J. R., Harpp, K. S., Hollocher, K., et al. (2013). Orogenic to postorogenic (1.20–1.15 Ga) magmatism in the Adirondack Lowlands and Frontenac terrane, southern Grenville Province, USA and Canada. *Geosphere*, *9*(6), 1637–1663. https://doi.org/10.1130/ges00879.1
Pfister, J. D., Kontak, D. J., & Marsh, J. H. (2023). Unraveling 800 Ma of pegmatite formation in the western Grenville Front tectonic Zone near Sudbury, Canada. *Precambrian Research*, *395*, 107128. https://doi.org/10.1016/j.precamres.2023.107128
Regan, S., Walsh, G., Williams, M., Chiarenzelli, J., Toft, M., & McAleer, R. (2019). Syn-collisional exhumation of hot middle crust in the Adirondack Mountains (New York, USA): Implications for extensional orogenesis in the southern Grenville province. *Geosphere*, *15*(4), 1240–1261. https://doi.org/10.1130/ges02029.1
Reynolds, P. H., Culshaw, N. G., Jamieson, R. A., Grant, S. L., & McKenzie, K. J. (1995). 40Ar/39Ar traverse-Grenville Front Tectonic Zone to Britt domain, Grenville Province, Ontario, Canada. *Journal of Metamorphic Geology*, *13*(2), 209–221. https://doi.org/10.1111/j.1525-1314.1995.tb00214.x

Rickard, L. V., & Fisher, D. W. (1975). *Correlation of the Silurian and Devonian rocks in New York state* (Vol. 24). University of the State of New York, State Education Department.

Rivers, T. (2008). Assembly and preservation of lower, mid, and upper orogenic crust in the Grenville Province—Implications for the evolution of large hot long-duration orogens. *Precambrian Research*, *167*(3–4), 237–259. https://doi.org/10.1016/j.precamres.2008.08.005

Rivers, T., Culshaw, N., Hynes, A., Indares, A., Jamieson, R., Martignole, J., et al. (2012). The Grenville orogen–A post-LITHOPROBE perspective. In *Tectonic styles in Canada: The lithoprobe perspective* (Vol. 49, pp. 97–236).

Rivers, T., & Volkert, R. A. (2023). Slow cooling in the metamorphic cores of Grenvillian large metamorphic core complexes and the thermal signature of the Ottawan orogenic lid. In *Laurentia: Turning points in the evolution of a continent*. Geological Society of America. https://doi.org/10.1130/2022.1220

Roden-Tice, M. K., & Tice, S. J. (2005). Regional-scale mid-Jurassic to late Cretaceous unroofing from the Adirondack Mountains through central New England based on apatite fission-track and (U-Th)/He thermochronology. *The Journal of Geology*, *113*(5), 535–552. https://doi.org/10.1086/431908

Rose, I. R., Zhang, Y., & Swanson-Hysell, N. L. (2022). Bayesian paleomagnetic Euler pole inversion for paleogeographic reconstruction and analysis. *Journal of Geophysical Research: Solid Earth*, *127*(10), e2021JB023890. https://doi.org/10.1029/2021jb023890

Schoene, B., & Bowring, S. A. (2007). Determining accurate temperature–time paths from U–Pb thermochronology: An example from the Kaapvaal craton, southern Africa. *Geochimica et Cosmochimica Acta*, *71*(1), 165–185. https://doi.org/10.1016/j.gca.2006.08.029

Selleck, B. W. (1980). The post-orogenic history of the Adirondack Mountain region: A review. *Geological Society of America Bulletin*, *91*(2), 120. https://doi.org/10.1130/0016-7606(1980)91⟨120:tphota⟩2.0.co;2

Seman, S., Stockli, D., & McLean, N. (2017). U-Pb geochronology of grossular-andradite garnet. *Chemical Geology*, *460*, 106–116. https://doi.org/10.1016/j.chemgeo.2017.04.020

Shinevar, W. J., Jagoutz, O., & Van Tongeren, J. A. (2021). Gore Mountain garnet amphibolite records UHT conditions: Implications for the rheology of the lower continental crust during orogenesis. *Journal of Petrology*, *62*(4), egab007. https://doi.org/10.1093/petrology/egab007

Slotznick, S. P., Swanson-Hysell, N. L., Zhang, Y., Clayton, K. E., Wellman, C. H., Tosca, N. J., & Strother, P. K. (2023). Reconstructing the paleoenvironment of an oxygenated Mesoproterozoic shoreline and its record of life. *GSA Bulletin*. https://doi.org/10.1130/B36634.1

Spear, F. S., & Markussen, J. C. (1997). Mineral zoning, P-T-X-M phase relations, and metamorphic evolution of some Adirondack granulites, New York. *Journal of Petrology*, *38*(6), 757–783. https://doi.org/10.1093/petroj/38.6.757

Storm, L. C., & Spear, F. S. (2005). Pressure, temperature and cooling rates of granulite facies migmatitic pelites from the southern Adirondack Highlands, New York. *Journal of Metamorphic Geology*, *23*(2), 107–130. https://doi.org/10.1111/j.1525-1314.2005.00565.x

Streepey, M. M., Lithgow-Bertelloni, C., van der Pluijm, B. A., Essene, E. J., & Magloughlin, J. F. (2004). Exhumation of a collisional orogen: A perspective from the North American Grenville Province. In *Proterozoic tectonic evolution of the Grenville orogen in North America*. Geological Society of America. https://doi.org/10.1130/0-8137-1197-5.391

Swanson-Hysell, N. L., Ramezani, J., Fairchild, L. M., & Rose, I. R. (2019). Failed rifting and fast drifting: Midcontinent Rift development, Laurentia's rapid motion and the driver of Grenvillian orogenesis. *GSA Bulletin*, *131*(5–6), 913–940. https://doi.org/10.1130/b31944.1

Swanson-Hysell, N. L., Rivers, T., & van der Lee, S. (2023). The late Mesoproterozoic to early Neoproterozoic Grenvillian orogeny and the assembly of Rodinia: Turning point in the tectonic evolution of Laurentia. In *Laurentia: Turning points in the evolution of a continent*. Geological Society of America. https://doi.org/10.1130/2022.1220

Taylor, J. P., & Fitzgerald, P. G. (2011). Low-temperature thermal history and landscape development of the eastern Adirondack Mountains, New York: Constraints from apatite fission-track thermochronology and apatite (U-Th)/He dating. *Geological Society of America Bulletin*, *123*(3–4), 412–426. https://doi.org/10.1130/b30138.1

Thieblot, L., Tequi, C., & Richet, P. (1999). High-temperature heat capacity of grossular (Ca3Al2Si3O12), enstatite (MgSiO3), and titanite (CaTiSiO5). *American Mineralogist*, *84*(5–6), 848–855. https://doi.org/10.2138/am-1999-5-618

Valentino, D. W., Chiarenzelli, J. R., & Regan, S. P. (2019). Spatial and temporal links between Shawinigan accretionary orogenesis and massif anorthosite intrusion, southern Grenville Province, New York, U.S.A. *Journal of Geodynamics*, *129*, 80–97. https://doi.org/10.1016/j.jog.2018.04.001

Valley, J. W., Bohlen, S. R., Essene, E. J., & Lamb, W. (1990). Metamorphism in the Adirondacks: II. The role of fluids. *Journal of Petrology*, *31*(3), 555–596. https://doi.org/10.1093/petrology/31.3.555

Valley, J. W., Chiarenzelli, J. R., & McLelland, J. M. (1994). Oxygen isotope geochemistry of zircon. *Earth and Planetary Science Letters*, *126*(4), 187–206. https://doi.org/10.1016/0012-821x(94)90106-6

Warnock, A. C., Kodama, K. P., & Zeitler, P. K. (2000). Using thermochronometry and low-temperature demagnetization to accurately date Precambrian paleomagnetic poles. *Journal of Geophysical Research*, *105*(B8), 19435–19453. https://doi.org/10.1029/2000jb900114

Weary, D. J., Ryder, R. T., & Nyahay, R. E. (2001). Thermal maturity patterns in New York State using CAI and %Ro. *Northeastern Geology and Environmental Sciences*, *23*(4), 356–376.

Weil, A. B., der Voo, R. V., Niocaill, C. M., & Meert, J. G. (1998). The Proterozoic supercontinent Rodinia: Paleomagnetically derived reconstructions for 1100 to 800 Ma. *Earth and Planetary Science Letters*, *154*(1–4), 13–24. https://doi.org/10.1016/s0012-821x(97)00127-1

Williams, M. L., Grover, T., Jercinovic, M. J., Regan, S. P., Pless, C. R., & Suarez, K. A. (2019). Constraining the timing and character of crustal melting in the Adirondack Mountains using multi-scale compositional mapping and in-situ monazite geochronology. *American Mineralogist*, *104*(11), 1585–1602. https://doi.org/10.2138/am-2019-6906

Zhang, Y., Anderson, N. S., Mohr, M. T., Nelson, L. L., Macdonald, F. A., Schmitz, M. D., et al. (2024). Paleomagnetic records from pulsed magmatism in the southwestern Laurentia large igneous province and Cardenas Basalt support rapid late Mesoproterozoic plate motion. *Journal of Geophysical Research: Solid Earth*, *129*(10), e2024JB029036. https://doi.org/10.1029/2024jb029036

Zhang, Y., Hodgin, E. B., Alemu, T., Pierce, J., Fuentes, A., & Swanson-Hysell, N. L. (2024). Tracking Rodinia into the Neoproterozoic: New paleomagnetic constraints from the Jacobsville Formation. *Tectonics*, *43*(2). https://doi.org/10.1029/2023TC007866

References From the Supporting Information

Aleinikoff, J. N., Wintsch, R. P., Tollo, R. P., Unruh, D. M., Fanning, C. M., & Schmitz, M. D. (2007). Ages and origins of rocks of the Killingworth dome, south-central Connecticut: Implications for the tectonic evolution of southern New England. *American Journal of Science*, *307*(1), 63–118. https://doi.org/10.2475/01.2007.04

Apen, F. E., Wall, C. J., Cottle, J. M., Schmitz, M. D., Kylander-Clark, A. R., & Seward, G. G. (2022). Apatites for destruction: Reference apatites from Morocco and Brazil for U-Pb petrochronology and Nd and Sr isotope geochemistry. *Chemical Geology*, *590*, 120689. https://doi.org/10.1016/j.chemgeo.2021.120689

Axelsson, E., Pape, J., Berndt, J., Corfu, F., Mezger, K., & Raith, M. M. (2018). Rutile R632—A new natural reference material for U-Pb and Zr determination. *Geostandards and Geoanalytical Research*, *42*(3), 319–338. https://doi.org/10.1111/ggr.12213

Gerstenberger, H., & Haase, G. (1997). A highly effective emitter substance for mass spectrometric Pb isotope ratio determinations. *Chemical Geology*, *136*(3–4), 309–312. https://doi.org/10.1016/S0009-2541(96)00033-2

Hayden, L. A., & Watson, E. B. (2007). Rutile saturation in hydrous siliceous melts and its bearing on Ti-thermometry of quartz and zircon. *Earth and Planetary Science Letters*, *258*(3–4), 561–568. https://doi.org/10.1016/j.epsl.2007.04.020

Housh, T., & Bowring, S. A. (1991). Lead isotopic heterogeneities within alkali feldspars: Implications for the determination of initial lead isotopic compositions. *Geochimica et Cosmochimica Acta*, *55*(8), 2309–2316. https://doi.org/10.1016/0016-7037(91)90106-F

Keller, C. B., McDannell, K. T., Guenthner, W., & Shuster, D. L. (2022). Thermochron.jl. https://doi.org/10.17605/OSF.IO/WQ2U5

Kennedy, A. K., Wotzlaw, J.-F., Crowley, J. L., Schmitz, M., Schaltegger, U., Wade, B., et al. (2023). Apatite reference materials for SIMS microanalysis of isotopes and trace elements. *Geostandards and Geoanalytical Research*, *47*(2), 373–402. https://doi.org/10.1111/ggr.12477

Kirschvink, J. L. (1980). The least-squares line and plane and the analysis of palaeomagnetic data. *Geophysical Journal International*, *62*(3), 699–718. https://doi.org/10.1111/j.1365-246x.1980.tb02601.x

Krogh, T. (1973). A low contamination method for the hydrothermal decomposition of zircon and extraction of U and Pb for isotopic age determinations. *Geochimica Cosmochimicha Acta*, *37*(3), 485–494. https://doi.org/10.1016/0016-7037(73)90213-5

Meng, J., Wu, S., Wang, H., Yang, Y., Huang, C., Zhang, C., et al. (2024). The KNW rutile—A natural reference material for microbeam U–Pb age and trace element determination. *Journal of Analytical Atomic Spectrometry*, *39*(10), 2488–2501. https://doi.org/10.1039/D4JA00190G

Pedersen, R. B., Dunning, G. R., & Robins, B. (1989). U-Pb ages of nepheline syenite pegmatites from the Seiland Magmatic Province, N. Norway. In *The Caledonides geology of Scandinavia* (pp. 3–8).

Rackauckas, C., & Nie, Q. (2017). DifferentialEquations.jl – A performant and feature-rich ecosystem for solving differential equations in Julia. *Journal of Open Research Software*, *5*(1), 15. https://doi.org/10.5334/jors.151

Rudge, J. F., Reynolds, B. C., & Bourdon, B. (2009). The double spike toolbox. *Chemical Geology*, *265*(3), 420–431. https://doi.org/10.1016/j.chemgeo.2009.05.010

Schaltegger, U., Ovtcharova, M., Gaynor, S. P., Schoene, B., Wotzlaw, J.-F., Davies, J. F. H. L., et al. (2021). Long-term repeatability and interlaboratory reproducibility of high-precision ID-TIMS U–Pb geochronology. *Journal of Analytical Atomic Spectrometry*, *36*(7), 1466–1477. https://doi.org/10.1039/D1JA00116G

Schwartz, D. M., Wanless, V. D., Schmitz, M. D., & Soule, S. A. (2019). Near-Linear relationship of double-spike corrected Pb isotope ratios of Galápagos lavas indicate formation from a single genetically linked recycled source. In *AGU fall meeting abstracts* (Vol. 2019).DI33C-0055.

Sláma, J., Košler, J., Condon, D. J., Crowley, J. L., Gerdes, A., Hanchar, J. M., et al. (2008). Plešovice zircon—A new natural reference material for U–Pb and Hf isotopic microanalysis. *Chemical Geology*, *249*(1–2), 1–35. https://doi.org/10.1016/j.chemgeo.2007.11.005

Spandler, C., Hammerli, J., Sha, P., Hilbert-Wolf, H., Hu, Y., Roberts, E., & Schmitz, M. (2016). MKED1: A new titanite standard for in situ analysis of Sm-Nd isotopes and U-Pb geochronology. *Chemical Geology*, *425*, 110–126. https://doi.org/10.1016/j.chemgeo.2016.01.002

Strelow, F. W. E., & Toerien, F. S. (1966). Separation of Lead(II), from Bismuth(III), Thallium(III), Cadmium(II), Mercury(II), Gold(III), Platinum(IV), Palladium(II), and other elements by anion exchange chromatography. *Analytical Chemistry*, *38*(4), 545–548. https://doi.org/10.1021/ac60236a006

Sun, S.-S., & McDonough, W. F. (1989). Chemical and isotopic systematics of oceanic basalts: Implications for mantle composition and processes. *Geological Society, London, Special Publications*, *42*(1), 313–345. https://doi.org/10.1144/gsl.sp.1989.042.01.19

Swanson-Hysell, N. L., Hoaglund, S. A., Crowley, J. L., Schmitz, M. D., Zhang, Y., & Miller, J. D. (2021). Rapid emplacement of massive Duluth Complex intrusions within the North American Midcontinent Rift. *Geology*, *49*(2), 185–189. https://doi.org/10.1130/g47873.1

Szymanowski, D., Wotzlaw, J.-F., Ovtcharova, M., Schoene, B., Schaltegger, U., Schmitz, M. D., et al. (2025). Interlaboratory reproducibility of ID-TIMS U–Pb geochronology evaluated with a pre-spiked natural zircon solution. *Geochronology*, *7*(3), 409–425. https://doi.org/10.5194/gchron-7-409-2025

Tauxe, L., Shaar, R., Jonestrask, L., Swanson-Hysell, N. L., Minnett, R., Koppers, A. A. P., et al. (2016). PmagPy: Software package for paleomagnetic data analysis and a bridge to the magnetics information consortium (MagIC) database. *Geochemistry, Geophysics, Geosystems*, *17*(6), 2450–2463. https://doi.org/10.1002/2016gc006307

Thirlwall, M. F. (2000). Inter-laboratory and other errors in Pb isotope analyses investigated using a 207Pb–204Pb double spike. *Chemical Geology*, *163*(1), 299–322. https://doi.org/10.1016/S0009-2541(99)00135-7

Wiedenbeck, M., Alla, P., Corfu, F., Griffin, W., Meier, M., Oberli, F., & Spiegel, W. (1995). Three natural zircon standards for U-Th-Pb, Lu-Hf, trace element and REE analyses. *Geostandards Newsletter*, *19*(1). https://doi.org/10.1111/j.1751-908x.1995.tb00147.x